



Guidelines for Voltage Stability Assessment on Systems with Large Integration of IBRs

Final Project Report

S-108G

Power Systems Engineering Research Center
*Empowering Minds to Engineer
the Future Electric Energy System*



Guidelines for Voltage Stability Assessment on Systems with Large Integration of IBRs

Final Project Report

Project Team

Amarsagar Reddy Ramapuram Matavalam, Project Leader

Anirudh Chatti Venkata Shesha

Arizona State University

PSERC Publication 24-08

December 2024

For information about this project, contact:

Amarsagar Reddy Ramapuram Matavalam
Arizona State University
School of Electrical, Computer, and Energy Engineering
Tempe, AZ, 85287
Email: amar.sagar@asu.edu

Power Systems Engineering Research Center

The Power Systems Engineering Research Center (PSERC) is a multi-university Center conducting research on challenges facing the electric power industry and educating the next generation of power engineers. More information about PSERC can be found at the Center's website: <http://www.pserc.org>.

For additional information, contact:

Power Systems Engineering Research Center
Arizona State University
527 Engineering Research Center
Tempe, Arizona 85287-5706
Phone: 480-965-1643
Fax: 480-727-2052

Notice Concerning Copyright Material

PSERC members are given permission to copy without fee all or part of this publication for internal use if appropriate attribution is given to this document as the source material. This report is available for downloading from the PSERC website.

© 2024 Arizona State University. All rights reserved.

Acknowledgments

We would like to express our gratitude to the project advisors for their technical feedback and insightful suggestions, particularly:

- Alberto Del Rosso, EPRI
- Mahendra Patel, EPRI
- Tamer Ibrahim, EPRI

Executive Summary

Large integration of renewable variable generation and inverter-based resources (IBR) alters the system's response to contingencies and fault events, and consequently the ability of the system to preserve stable operation under critical conditions. Renewables and IBRs affect voltage stability in various ways, and consequently There is an urgent need to reevaluate stability assessment methods for Transmission and Distribution (T&D) systems with high penetration IBRs.

The inherent uncertainty associated with IBRs significantly impacts both short- and long-term voltage stability. A critical challenge in this context is the accurate modeling of IBRs for stability assessments, as it requires a comprehensive understanding of their interactions with system dynamics. Additionally, the volt-var control (VVC) produces the reactive power and enables IBRs to participate in voltage regulation within distribution systems. Therefore, replicating the reactive support capabilities of IBRs in stability studies is crucial, as it can significantly enhance the reliability of both transmission and distribution networks.

The work evaluated the stability of T&D systems under significant integration of IBRs. Two approaches were employed for the stability assessment: a T&D co-simulation framework and an aggregated model representation. The co-simulation approach utilized detailed modeling of the distribution network, capturing the effects of imbalances, resulting in a reduced voltage stability margin (benchmark for comparison). In contrast, the aggregated models provided a conservative and optimistic stability margin by overlooking the intricate details of the distribution networks. In addition to this, we developed an aggregated model to incorporate the VVC into stability, which yielded an optimistic estimate of the stability margin. Notably, the inclusion of VVC in the aggregated models resulted in a good voltage match with the T&D co-simulation studies.

Major outcome of the analysis is that the aggregated model used for voltage stability assessment effectively estimates the stability margin of IBR-rich grids. Regardless of varying load models in the distribution network, the aggregated model consistently produces conservative or optimistic results, remaining close to the true margin. Moreover, if transmission operators set the voltage threshold to 0.9 p.u. for stability assessment, incorporating VVC in the aggregated models achieves comparable accuracy to the T&D co-simulation.

Project Publications (All the Manuscripts are under preparation):

- [1] Anirudh C.V.S and Amarsagar Reddy Ramapuram Matavalam "Evaluating the Impact of IBR Volt-VAR Control on Voltage Stability through QV Analysis," *IEEE Transactions on Power Systems*.
- [2] Anirudh C.V.S and Amarsagar Reddy Ramapuram Matavalam "Impact of Distribution System Strength on Voltage Stability Assessment in IBR-Rich Grids," *IEEE Transactions on Power Systems*.
- [3] Anirudh C.V.S and Amarsagar Reddy Ramapuram Matavalam "Enhanced Aggregated Models for Voltage Stability Assessment through PV Analysis," *IEEE Transactions on Power Systems*.

Table of Contents

1. Introduction.....	1
1.1 Overview	1
1.2 Overview of the Problem.....	1
1.3 Objective of the work	3
1.4 Report Organization	4
2. Background.....	5
2.1 Introduction	5
2.2 Power System Planning Studies	5
2.3 Voltage Stability Assessment Studies	6
2.4 Transfer Capability Studies	6
2.4.1 Case Study with Simple Two Bus System	8
2.5 Modeling of T&D Systems for Stability Studies	10
3. Research Methodology	11
3.1 Introduction	11
3.2 T&D Co-simulation Framework	11
3.3 Impact of Load Increment on Distribution Systems.....	12
3.3.1 Impact of Load Models on Distribution System	16
3.4 Impact of Load Increment on Distribution Systems.....	19
3.5 T&D Co-simulation Framework for PV Analysis.....	22
3.6 Aggregated Model for PV Analysis	24
3.6.1 Nominal Load Computation for Aggregated Models.....	24
3.6.2 Incorporation of VVC into Aggregated Models.....	26
4. Results and Discussions.....	30
4.1 Analysis of IEEE 9-bus and IEEE 123 Node Distribution System	31
4.1.1 Impact of DER on Stability Assessment	33
4.2 Analysis of IEEE 240 WECC and IEEE 123 Node Distribution System	38
4.3 Analysis of System X and IEEE 123 Node Distribution System.....	40
4.3.1 Results for Constant Impedance Loads	41
4.3.2 Results for Constant Current Loads	42
4.3.3 Results for Constant Power Loads	43
5. Conclusions.....	46

5.1 Guidelines for Performing Voltage Stability Assessment.....	46
5.2 Future Work.....	47
Appendix A Comparison with TDcoSim.....	48
Appendix B Strengthening of Distribution Networks for Stability Studies	51
References.....	53

List of Figures

Figure 1.1 Active D-sys with DERs, ESS and network management.	2
Figure 1.2 Multiple active distribution networks connected to transmission network.	3
Figure 2.1 Typical transmission planning studies for voltage stability studies [12].	5
Figure 2.2 Schematic representation of load increment.....	7
Figure 2.3 Typical PV curve of a bus obtained by increasing the loads.....	7
Figure 2.4 Simple two bus system considered for PV analysis.	8
Figure 2.5 PV curve corresponding to Case A.	9
Figure 2.6 PV curve corresponding to Case B.....	9
Figure 2.7 Schematic representation of T&D co-simulation.	10
Figure 3.1 Generic framework for T&D co-simulation.....	11
Figure 3.2 General schematic representation of load increment in the D-sys.	12
Figure 3.3 Real power variation with λ	13
Figure 3.4 Reactive power variation with λ	13
Figure 3.5 Variation of losses in distribution system.	14
Figure 3.6 Variation of power factor at substation.	14
Figure 3.7 Tap positions inside D-sys.....	15
Figure 3.8 Variation of impedance at substation.	16
Figure 3.9 Real power seen at substation for different load models in D-sys.	17
Figure 3.10 Reactive power seen at substation for different load models in D-sys.....	17
Figure 3.11 Reactive losses of D-sys.....	18
Figure 3.12 Power factor seen at substation.	18
Figure 3.13 Variation of real power at substation in presence of DER.	20
Figure 3.14 Typical VVC curve of SPV.....	21
Figure 3.15 Variation of VAR power from DERs as a function of DER node voltage.....	21
Figure 3.16 General schematic for feeder increment method.....	23
Figure 3.17 Flowchart illustration T&D co-simulation process for obtaining PV curves.....	23
Figure 3.18 Aggregated model for stability studies.....	24
Figure 3.19 Step by step procedure to obtain nominal loading of aggregated model.	25
Figure 3.20 Aggregated model at UPF mode.	26
Figure 3.21 Aggregated model with VAR support (Agg.Model w VVC).....	26
Figure 3.22 Typical VVC curve of DER.	27

Figure 3.23 Lookup table approach to mimic VVC.	27
Figure 4.1 Framework for comparison of co-simulation studies and aggregated models.	30
Figure 4.2 PV curve with respect to λ as x-axis.	31
Figure 4.3 Variation of reactive power with respect to λ as x-axis.	32
Figure 4.4 PV curve with respect to PT as x-axis.	32
Figure 4.5 PV curve with respect to ΔPT as x-axis.	33
Figure 4.6 PV curve with respect to PT as x-axis under DER penetrations.	34
Figure 4.7 PV curve with respect to ΔPT as x-axis under DER penetrations.	34
Figure 4.8 Variation of power factor seen at substation.	35
Figure 4.9 PV curve with respect to ΔPT as x-axis under DER penetrations.	36
Figure 4.10 PV curve for IEEE 9 Bus-123 Node system with VVC enabled.	37
Figure 4.11 Detailed view of Bus 6401 within the 240 WECC System [35].	38
Figure 4.12 PV curve obtained for 240 WECC under different DER penetration scenarios.	39
Figure 4.13 HV side voltage for 50% DER scenario.	41
Figure 4.14 LV side voltage for 50% DER scenario.	41
Figure 4.15 LV side voltage for 25% DER scenario.	42
Figure 4.16 LV side voltage for 50% DER scenario.	43
Figure 4.17 HV side voltage for 25% DER scenario.	44
Figure 4.18 HV side voltage for 50% DER scenario.	44
Figure A.1. PV curve corresponding to Case-A.	48
Figure A.2 PV curve corresponding to Case-B.	49
Figure A.3 PV curve corresponding to Case-C at Bus 7.	49
Figure A.4 PV curve corresponding to Case-C at Bus 5.	50
Figure B.1 PV Curve for the IEEE 9-bus system and unstrengthened IEEE 123 node distribution network.	51
Figure B.2 Strengthening of the distribution network for stability studies.	52

List of Tables

Table 3.1 Impact of substation voltages on the load increment parameter.....	19
Table 3.2 Impact of VVC on the distribution system (Powers are expressed in p.u. with 100 MVA base).....	22
Table 4.1 Distribution systems connected to transmission buses for stability assessment.....	30
Table 4.2 DER capabilities considered for analysis of IEEE 9-bus and IEEE 123 node distribution system.....	34
Table 4.3 Impact of DER penetration at the T&D interface.....	35
Table 4.4 Maximum load handled in distribution network under co-simulation	36
Table 4.5 Incremental transfer power [in MW] under different DER scenarios	36
Table 4.6 Maximum incremental transfer obtained with different models	37
Table 4.7 DER capabilities considered for stability study of 240 WECC – IEEE 123 node system	38
Table 4.8 Incremental transfer power [in MW] under different DER penetration.	40
Table 4.9 DER capabilities consider for stability study of System X and IEEE 123 node system	40
Table 4.10 Max. ΔP_T [in MW] from different studies with constant impedance loads	42
Table 4.11 Max. ΔP_T [in MW] from different studies with constant current loads	43
Table 4.12 Max. ΔP_T [in MW] from different studies with constant power loads	44

1. Introduction

1.1 Overview

Large integration of renewable variable generation and inverter-based resources (IBR) alters the system's response to contingencies and fault events, and so the ability of the system to preserve stable operation under critical conditions. Renewables and IBRs affect voltage stability in numerous ways, and consequently the methodologies and simulation tools used for the assessment of voltage stability and control. To address these challenges, this project develops practical guidelines for power system operation and planning engineers to perform voltage stability assessment in transmission systems, especially in conditions where large penetration of IBRs (in the transmission and distribution grids) affects the behavior and response of the bulk power system (BPS). This project is intended to initiate the development and implementation of various improved methodologies and tools for voltage stability assessment.

1.2 Overview of the Problem

The power system is a complex network comprising generation, transmission, and distribution components. Bulk power is generated and transmitted through high-voltage corridors to lower-level distribution systems. This grid spans multiple regions and countries, with operating conditions that are continually evolving. A critical aspect of this network is voltage stability, which presents significant challenges and necessitates careful management. To ensure the effective and reliable operation of bulk power systems, a range of planning and operational studies are conducted. Voltage stability has long been recognized as a fundamental concern, leading to extensive research aimed at defining its concept and implications [1]-[5]. The stability of the power system can manifest in various forms and can be managed through multiple strategies. Consequently, numerous methodologies and tools have been developed by utilities and academic institutions to assess stability. The planning and operational studies focused on this assessment aim to maintain satisfactory voltage levels throughout the grid. Most of these studies primarily focused on how the transmission control operations impacted the power distributed networks. This part of assumption was valid if the distribution systems are passive, and the behavior is well known in front.

In recent decades, the energy transition has seen significant integration of renewable energy sources, particularly solar and wind, with expectations for rapid acceleration [6]. This integration at the transmission level has improved network performance, enhancing ride-through capabilities and system stability. Advancements in power electronics have also enabled the incorporation of inverter-based resources (IBRs) at sub-transmission and distribution levels. IBRs make the distribution network more active Figure 1.1, significantly impacting overall performance due to increased transmission-distribution (T&D) interactions. Moreover, IEEE Std 1547 [7] mandates that IBRs provide ancillary services during adverse operating conditions.

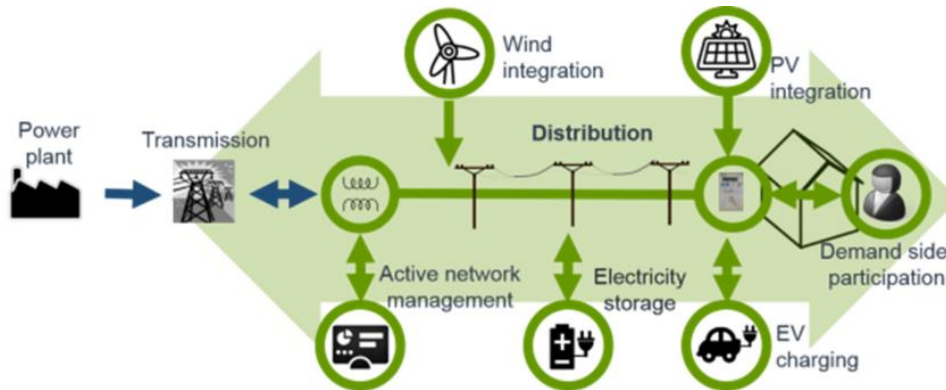


Figure 1.1 Active D-sys with DERs, ESS and network management.

Several joint task forces and working groups were formed to address how the stability of the modern power grids is impacted by the intermittent nature of IBRs [8][9]. EPRI report [10] highlights the limitations of the current practices used for voltage stability assessment of IBR dominated grids. The studies emphasized the need to investigate stability assessment methods for Transmission and Distribution (T&D) systems with high IBR penetration. The uncertainty of IBRs affects both short and long-term voltage instability, with system responses varying significantly based on power injection profiles, and potentially incompatible with equally likely samples. Beyond the uncertainty, modeling of the IBRs for stability assessment is a key challenge as this requires deep insight of IBRs interactions with the system logic. Furthermore, from a planning point of view, it is crucial to define the level of precise IBR modeling required for performing accurate stability analysis.

IBRs operating modes change the system dynamics over a period, making stability assessment critical. Due to the inverter control logic, along with real power, IBRs can produce reactive power depending on the individual IBR capacity. This aspect of VAR support from IBR allows it to actively take part in the voltage regulation of the distribution systems [11]. The replication of reactive support from IBRs for stability studies is essential as it can enhance reliability of both transmission and distribution networks. To replicate this level of detailing in the planning studies, one must understand the following aspects:

1. How does the VAR support from IBRs interact with the existing control logics of distribution systems? The distribution network consists of tap changers and capacitor banks to regulate the voltages and power factor. With the increased IBR participation, it is needed to understand how these controls get effected.
2. To what extent the IBRs are dispersed in the distribution system? The reactive power support of IBR depends on the voltage seen at the DER node. The support greatly relies on the distribution network configuration. Even if the IBRs are situated near to substation buses, one cannot expect full VAR support from IBRs as it depends on the voltage droop characteristics of the inverter control curve.

In this direction, the work aims to evaluate the stability assessment of T&D systems under bulk penetration of IBRs. The focus of the work is to quantify to what extent the modeling of the IBRs is needed in the bulk planning studies and provide guidelines for performing the desired stability studies under higher penetration of DERs especially with reactive power support from the DERs.

1.3 Objective of the work

The impact of distribution networks on system stability can only be accurately assessed through detailed modeling of the distribution system. This is accomplished via T&D co-simulation studies, which involve comprehensive modeling of distribution systems. Traditionally, planning studies have utilized aggregated models, representing distribution systems as consolidated loads at transmission buses. This approach was effective when distribution networks were passive and net load characteristics were predictable. However, with the increasing power support from inverter-based resources (IBRs) at various operating levels, the assumption of passive distribution networks is no longer valid, necessitating significant updates to the stability tools used for power system planning studies.

It remains unclear among planners and operators whether to adopt T&D co-simulation studies extensively or to parameterize aggregated models for power system planning. If parameterized models are to be used for stability assessments, utilities must consider the additional challenges of implementation and whether these new aggregated models adequately capture the critical features of distribution systems. Ultimately, this situation presents a trade-off between computational complexity and the accuracy of estimating the stability margins of IBR-rich T&D systems. The objective of this work is threefold:

1. How good is the aggregated model compared to that of T&D co-simulation?
2. Does the nature of loads in the D-sys impact the stability of the system? If so, to what extent is the stability margin impacted and how to parameterize the aggregated model?
3. Is it possible to rely on aggregated model simulation under higher IBR penetrations, especially when IBRs are providing VAR support?

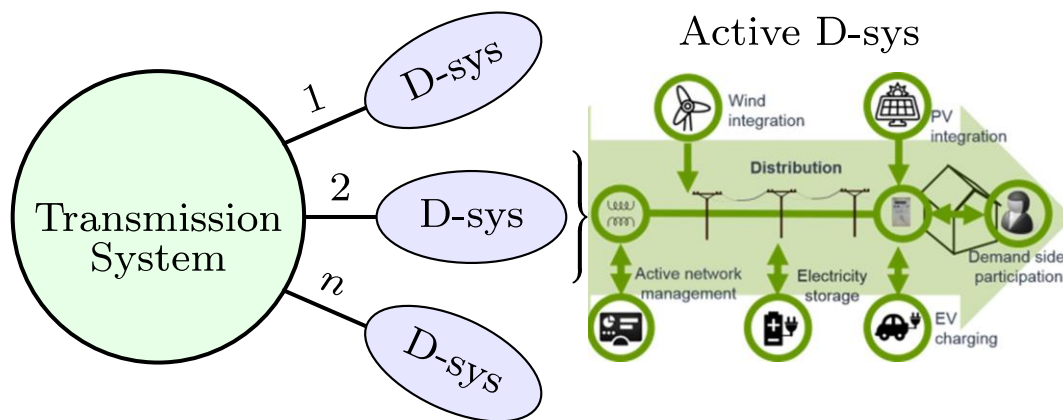


Figure 1.2 Multiple active distribution networks connected to transmission network.

The project aims to address these critical questions in the context of multiple low-level distribution systems connected to a transmission network (Figure 1.2). By analyzing the implications of various modeling approaches, the project seeks to identify the most effective methods for assessing system stability in this evolving landscape. Based on the findings, comprehensive guidelines will be provided to facilitate stability assessments of systems with

significant integration of IBRs. These guidelines will help utilities navigate the complexities associated with modeling and implementing appropriate strategies to ensure reliable system planning.

1.4 Report Organization

The report is structured into five sections.

Chapter 2 provides the theoretical background and outlines the methodologies related to transfer capability studies and T&D co-simulation.

Chapter 3 of the report outlines the working methodology and framework for conducting stability assessments using the co-simulation and aggregated model approach. It also examines the influence of load models and IBRs on distribution networks. Additionally, this section presents a framework for integrating VAR support from IBRs into the aggregated model for stability assessment.

Chapter 4 of the report presents the results obtained from various test scenarios utilizing co-simulation and aggregated models for stability assessment.

Finally, Chapter 5 offers conclusions and guidelines related to stability assessment.

2. Background

2.1 Introduction

Power system planning studies are essential for ensuring the grid's stability, efficiency, and dependability. They are critical in identifying possible stability concerns and developing mitigation techniques, such as voltage stability studies to assure reliable power transfer across different areas of the power grid. There are several approaches used for stability assessment of the power grid, and most of the methods do not account for the distribution system characteristics. There is a pressing need for new techniques to completely characterize IBRs behavior in stability studies as they become more common and unpredictable. The incorporation of transmission and distribution (T&D) co-simulation will help with long-term planning by providing a comprehensive perspective of distribution network interactions, assuring reliable grid operations.

2.2 Power System Planning Studies

Power system planning studies are conducted to ensure stable, efficient and reliable operation of the grid. The planning process and studies of power systems can be broadly classified into long-term studies, operational studies and real time operations. A typical simulation study of the planning process is shown in Figure 2.1. The key point of the planning process is to find the scenarios that might cause stability issues in the grid, followed by identifying the solutions to mitigate the instability scenarios [12]. To alleviate the undesirable voltage conditions, network reinforcements will be identified as a decisive step of the planning process.

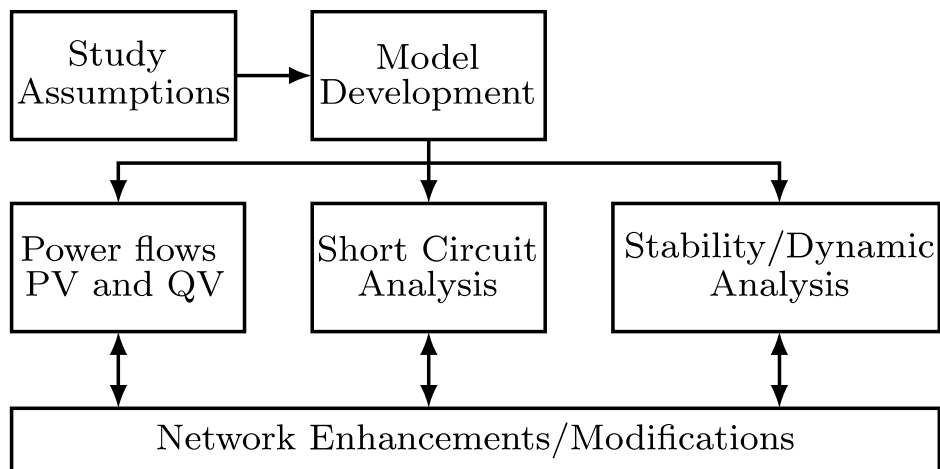


Figure 2.1 Typical transmission planning studies for voltage stability studies [12].

Typically, planning studies begin with the formulation of plausible future scenarios. Models of future transmission systems are created to do simulation studies using various inputs on projected system conditions. Grid models for power flow, dynamics, short circuit, and EMT studies are created based on future load and generation forecasts, transmission network topology, components, and expected reinforcements. For the planning studies, most utilities confine to steady-state stability assessment i.e., load-flow studies, PV analysis (transfer capability studies)

and QV analysis. This is due to lack of open-source platform for stability studies and rigidity on the point of view of system stability made to explore limited set of tools for stability assessment [10]. However, due to the unpredictable behavior of IBRs (and shut down of inertial resources), there is a need for new methodologies and unified models for performing stability assessment of BPS. The unified (aggregated) models developed should replicate the unpredictable behavior of IBRs to some extent to facilitate long-term planning studies.

2.3 Voltage Stability Assessment Studies

The voltage stability assessment of power systems has been a long-standing practice crucial for ensuring the reliable operation of the grid. Various tools and methodologies have been developed for this purpose, with a comprehensive summary of these tools available in references [[13],[14],[15]]. Voltage stability is categorized into short-term (lasting a few seconds) and long-term (spanning several minutes). Literature indicates power flow studies are adequate for conducting long-term stability assessments. As the power flow solutions are based on time-independent equations, this requires minimal data and can be scaled to larger systems with relatively low computational effort. Due to this, utilities are interested in static stability assessment of the power system and additionally, the CIGRE/IEEE joint taskforce [16] has identified that steady-state analysis (PV/QV analysis and power flow solutions) is the most adopted practice for planning studies.

Static stability analysis deals with determining the loadability limits of the power system and aims to determine what amount of load that can be delivered without compromising the system's stability. The developed methods for stability assessment fall under the category of model based and model free methods. Model-free (and hybrid) methods are utilized for online long-term voltage stability analysis, relying on data measurements from PMUs and SCADA, alongside power system models [17]-[20]. Academic researchers have reported machine learning-based voltage stability assessments [21], leveraging voltage stability properties to select appropriate features for various analytical techniques. Model-based methods [[24],[25]] employ the analytical network model for stability assessment, proving effective in identifying critical nodes or areas that may lead to voltage instability. Popular model-based methods include the continuation power flow (CPF) technique, Jacobian methods, and admittance matrix methods.

The CPF technique [[24]] is widely used to compute the stability margin of the grid. This method builds up the stress on the power system using a continuation parameter, solving the power flow until the point of divergence is reached. An alternative approach for determining the stability margin involves conducting a transfer capability study (PV curve analysis) by successively running the power flow solution until divergence occurs. Both methods incrementally increase the loads in a system area, helping planners identify the maximum transfer capability between loads and generators. The point of divergence signifies the load profile at which a valid system solution no longer exists; any further load increase beyond this point can lead to system collapse.

2.4 Transfer Capability Studies

In terms of planning for BPS, the transfer capability study (PV curve) is of key importance as it gives a picture of how much power can be transferred across different areas of transmission system

without compromising system stability. Outcome of this study determines how much incremental MW is possible prior to system instability. Furthermore, the capability study highlights the constraints that limit power transfer within the network. This allows system planners to identify solutions such as network enforcement or generation increments. The importance of the PV curve assessment and the factors that influence the transfer limit is detailed by EPRI [26].

A transfer capability study involves the analysis of power-voltage (PV) curves to evaluate the relationship between the power transfer and voltage stability within the power system. The PV curve is obtained through a series of load flow solutions, which involve defining sinks (loads) and sources (generators) of a transmission network.

The general schematic to perform the load increment for a transmission network is shown in Figure 2.2, where the loads at the desired buses or zones are changed to $S' = S(1 + \lambda)$, where λ is the load increment parameter. The real power generation at desired buses is adjusted accordingly for each MW increment in the load, followed by a load flow analysis.

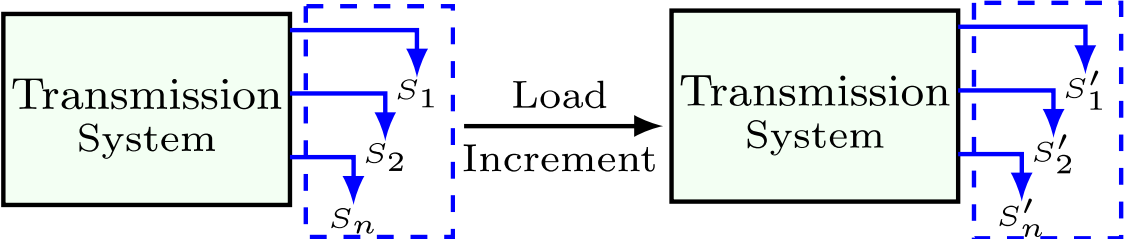


Figure 2.2 Schematic representation of load increment.

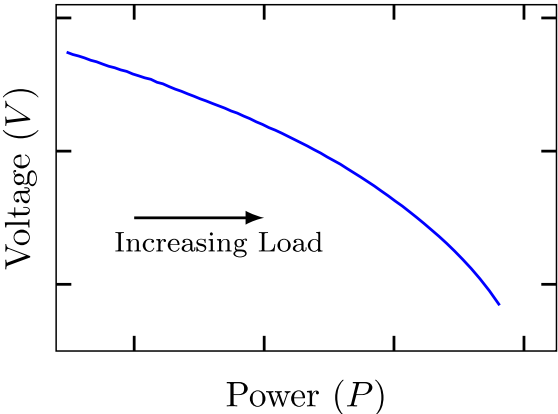


Figure 2.3 Typical PV curve of a bus obtained by increasing the loads.

A typical PV curve resulting from load increments at a particular bus is shown in Figure 2.3. This demonstrates how voltage magnitude at that bus varies as load power increases. As the system load increases, the voltage magnitude decreases, ultimately reaching a critical minimum known as the nose point of the PV curve. This nose point, or knee point, signifies the maximum power

transfer capability (maximum power margin) before the system approaches instability. Any further increment beyond this point risks system collapse, making it essential for accurately estimating the transfer margin. The nose point indicates the boundary between stable and unstable operating conditions. If the system operates beyond this point, it may lead to voltage collapse. An observation of Figure 2.3 indicates that PV curve exhibits significant non-linearity, which prevents the use of conventional sensitivity methods for its analysis. Consequently, a comprehensive series of load flow solutions is required to determine the power system's transfer capability accurately. Several commercial software packages, such as PSS/E, DIgSILENT PowerFactory, and PowerWorld, include built-in modules for conducting transfer capability studies and generating detailed analytical reports.

2.4.1 Case Study with Simple Two Bus System

In this section, we will try to demonstrate the importance to evaluate the transfer capability of system in the presence of IBRs with a simple two bus test system (shown in Figure 2.4). Bus-A is a slack bus and connected to load Bus-B via a line of reactance 0.2 p.u.. There are two loads S_L and S_D at Bus-B. S_L is fixed load bus with 100 MW real power demand operating at 0.9 power factor. S_D is a negative load of 50 MW (50% of P_L) considered to represent the DER capability at transmission level. Following two case studies are considered to demonstrate the impact of S_D on transfer capability:

1. Case A: When S_L is purely real and operated with $S_D = 0$ MW and $S_D = 50$ MW.
2. Case B: When S_L is operating at 0.9 lagging power factor ($Q_L = 48$ MVAR) and operated with $S_D = 0$ MW and $S_D = 50$ MW.

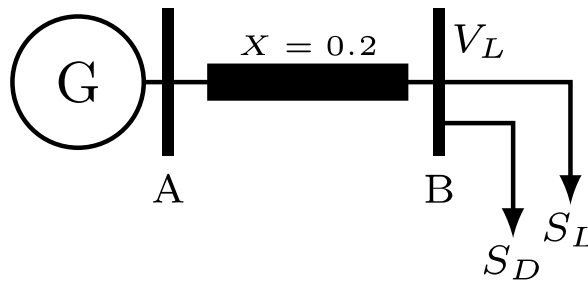


Figure 2.4 Simple two bus system considered for PV analysis.

The typical PV curves generated using the PSS/E-Python interface for this scenario are presented in Figure 2.5 and Figure 2.6, where P_T represents the net power observed at the load bus. In both cases, the injection of S_D leads to a substantial increase in the load bus voltage.

In Case A (Figure 2.5), the inclusion of S_D decreases the net load perceived by the transmission system, resulting in an increase of 50 MW in the transferable load capacity. This indicates a more efficient utilization of the available power.

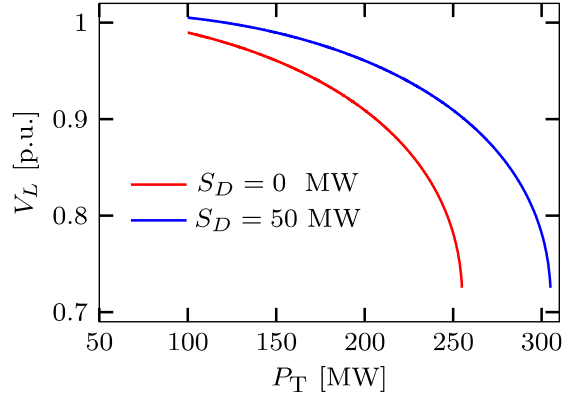


Figure 2.5 PV curve corresponding to Case A.

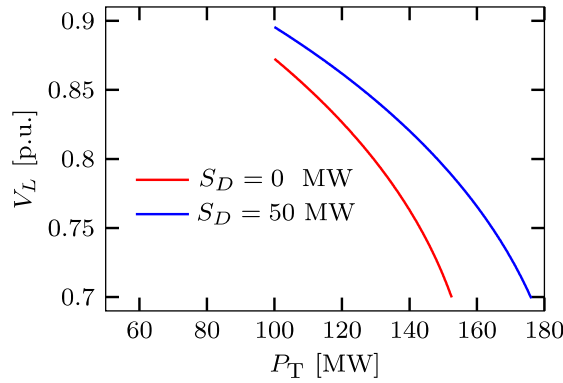


Figure 2.6 PV curve corresponding to Case B.

Conversely, in Case B (Figure 2.6), the load bus voltage V_L experiences a significant reduction due to a lower power factor, contrasting with Case A, which operates at unity power factor. The injection of S_D effectively lowers the real power seen by the transmission system while leaving the reactive power unchanged, which in turn enhances V_L . However, the increased reactive power demand in Case B leads to a marked reduction in the transfer margin compared to Case A. This highlights the critical impact of power factor on system stability and transfer capabilities.

The key takeaway from this illustration is that the transfer capability of the system is affected by the presence of IBRs, with limits dependent on the system's load. Higher reactive loads significantly influence power transferability, making it crucial to evaluate the impact of IBRs on PV assessments. Most transfer capability and stability studies assume the distribution network consists of aggregated loads at the transmission level, a valid approach for passive distribution networks. However, with the rise of active distribution networks, existing stability assessment tools need reevaluation. Additionally, distribution systems are often unbalanced, which significantly affects grid stability assessments. Capturing the true transferability margin in real-time unbalanced distribution systems presents a challenge. To fully understand the impact of the distribution network, T&D co-simulation studies are conducted.

2.5 Modeling of T&D Systems for Stability Studies

With the growing trend of active distribution networks, Independent System Operators (ISOs) and utilities are increasingly interested in integrating full-scale distribution systems into stability assessments. This integration is achievable through comprehensive transmission and distribution (T&D) co-simulation studies. These studies involve the seamless integration of transmission and distribution solvers on a single platform, allowing for a more accurate and holistic analysis of system stability.

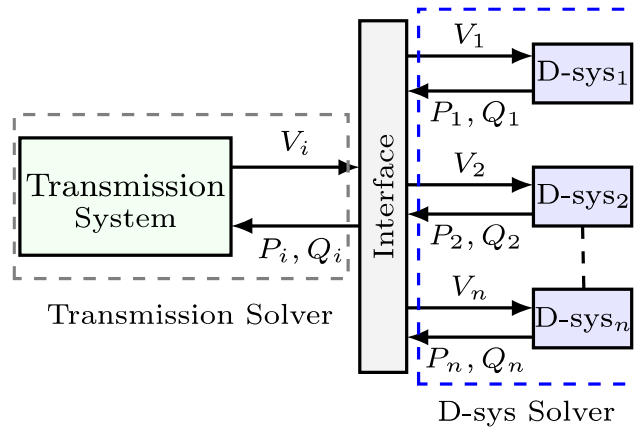


Figure 2.7 Schematic representation of T&D co-simulation.

T&D co-simulation provides a detailed model of both transmission and distribution systems. A generic framework for T&D co-simulation is illustrated in Figure 2.7. The transmission system is solved using transmission solvers such as PSS/E, PSLF, or PyPower. The distribution system (hereafter referred to as D-sys) is addressed using distribution simulators like OpenDSS, Helix, or GridLAB-D. Variables between the solvers are exchanged using an interface, which typically serves as a coding platform and primarily acts as a communicator between the T&D solvers. Tight coupling is ensured between the T&D systems, meaning the solvers continue to operate until they meet a voltage convergence criterion for a given operating point. It is important to note that T&D co-simulation heavily relies on the granularity of the D-sys model available and computationally intensive.

Full-scale distribution system modeling to assess the impact of active distribution systems on T&D systems has been successfully implemented [27]-[30], generating significant interest among academia and utilities in T&D co-simulation studies for stability analysis. This has also led to the development of an open-source platform for conducting static and dynamic assessments using T&D co-simulation frameworks [31],[32]. Voltage stability assessments utilizing T&D co-simulation have shown [[29],[30] that the unbalance in the distribution network significantly affects the stability margin. Additionally, reactive power support from IBRs has been shown to enhance the stability margin, a benefit that conventional aggregated models may overlook.

3. Research Methodology

3.1 Introduction

The growth of active distribution networks necessitates a new methodology to understand the complex interactions between T&D systems. The intermittent nature of IBRs and their interactions with various control actions within distribution networks (D-sys) present challenges in assessing their impact on T&D interactions. The co-simulation technique effectively evaluates these impacts, enabling a comprehensive analysis of how distribution networks influence T&D dynamics and capturing the key characteristics of D-sys.

3.2 T&D Co-simulation Framework

The T&D framework for stability analysis enables us to capture the details of D-sys. These details include the effects of unbalances, tap-changing actions, capacitor actions of D-sys, and distributed energy resources (DER). The inclusion of the T&D framework results in accurate margin assessment. However, a major drawback of T&D co-simulation is its computational complexity. The general framework of the T&D co-simulation is shown in Figure 3.1.

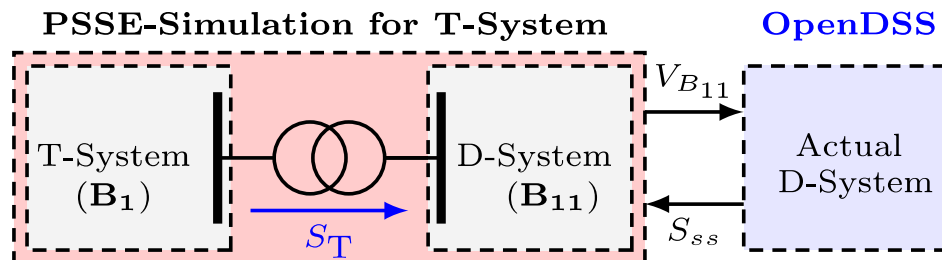


Figure 3.1 Generic framework for T&D co-simulation.

The transmission (T-) system is represented by a high-voltage bus (B_1), modeled in PSS/E, while the low-voltage distribution bus (B_{11}) is connected to B_1 through a transformer with reactance X_T . The transmission system is modeled as a positive sequence network. The entire distribution system is modeled in OpenDSS, an open-source distribution solver developed by EPRI for analyzing electric distribution systems. This approach provides a detailed model of the D-sys and effectively captures the impact of unbalances through co-simulation.

Both PSS/E and OpenDSS are accessed and automated using a Python coding environment, which serves as an interface between the two solvers. The variables exchanged between PSS/E and OpenDSS include the substation voltage ($V_{ss} = V_{B_{11}}$) and the total power at the substation (S_{ss}), which is represented as a constant PQ load in PSS/E at bus B_{11} . The net power at the substation is the sum of individual phase powers, expressed as $S_{ss} = S_a + S_b + S_c$, accounting for the total load and losses in the system. This co-simulation method allows for the consideration of unbalanced power in distribution networks at the transmission level.

Co-simulation terminates when the difference in substation voltages between consecutive iterations falls below a threshold of 10^{-5} . This methodology enables the capture of key parameters such as tap positions, total capacitor injections, total load, and total losses of the D-sys across various operating voltages. It is important to note that the loading of the D-sys typically operates at a few kW, while the load at the transmission bus is in the megawatt (MW) range. To effectively emulate a load equivalent to the transmission level, the load of the D-sys must be scaled appropriately to impact the overall T&D networks. This scaling is achieved by considering parallel feeders (N_f), determined based on the initial load observed at the transmission bus. Thus, for the co-simulation study, the effective load at bus B_{11} is represented as $N_f S_{SS}$. This loading level induces stress at the transmission level, which is reflected in the substation voltage ($V_{B_{11}}$), significantly impacting the distribution network under varying operating conditions.

3.3 Impact of Load Increment on Distribution Systems

This section aims to examine the behavior of the D-sys under different stress levels. The losses in the D-sys are inherently non-linear and are influenced by the loading level and the substation voltage of the system. Additionally, the voltage level within the D-sys dictates the tap actions and capacitance injections. The D-sys comprises various load models, specifically constant Z (impedance), constant I (current), and constant PQ (power) models. Each of these load models exerts a different degree of stress on the system.

Constant power loads stress the D-sys to greater extent when compared to that of the Constant impedance loads, as these loads are independent on the bus voltage to which they are connected. Another crucial factor is the unequal distribution of loads across the phases of the D-sys, which is likely to lead to significant unbalances as the loading level increases.

In this analysis, we will investigate how the power observed at the substation (S_{SS}), losses (S_{loss}), load (S_L), tap positions, and power factor at substation vary as stress within the D-sys escalates.

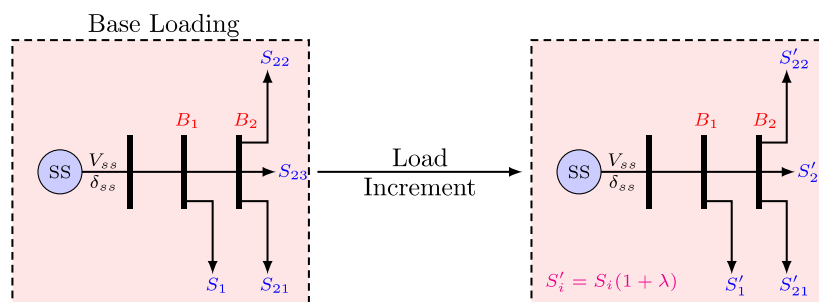


Figure 3.2 General schematic representation of load increment in the D-sys.

The D-sys model is implemented in OpenDSS software through a Python interface. The loads of the D-sys are accessed using OpenDSSDirect commands. The generic approach to increase the load in the D-sys is shown in Figure 3.2. For a sample D-sys operating under base loading conditions, let V_{SS} represent the substation voltage, and $S_i (= P_i + jQ_i)$ denote the load at the i^{th} bus of the D-sys.

Both real and reactive loads are increased by a load increment parameter λ , given by (3.1).

$$S'_i = P'_i + jQ'_i = P_i(1 + \lambda) + jQ_i(1 + \lambda) \quad (3.1)$$

It is important to note that the λ increment depends on the type of load model in the D-sys. Load increment in D-sys is done using Load Mult command of OpenDSS software. The system is solved in snap-shot mode with the new loading scenario till the point of divergence.

To assess the impact of load increment on the D-sys, the aforementioned methodology is implemented for the IEEE 123 node distribution network without any co-simulation. For this study, a load increment parameter of $\lambda = 1\%$ is used, while the substation voltage is maintained at 1 p.u. throughout the simulation analysis. Constant power loads are considered in the D-sys, and $N_f = 20$ is used to scale the powers obtained from OpenDSS. Additionally, all power values are expressed in per unit (p.u.) on a 100 MVA base.

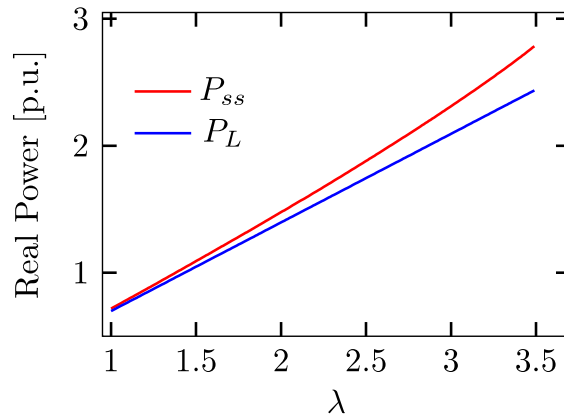


Figure 3.3 Real power variation with λ .

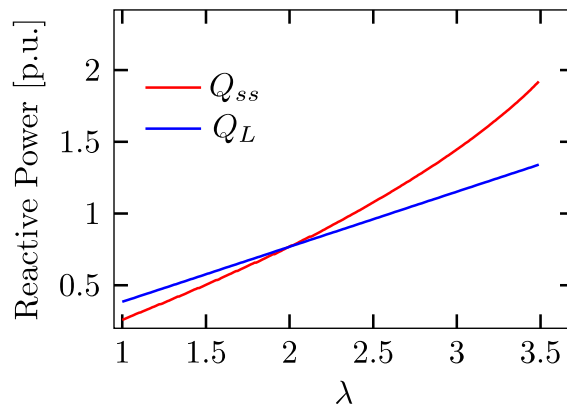


Figure 3.4 Reactive power variation with λ .

Figure 3.3 and Figure 3.4 demonstrates the variation of real and reactive power within the system as the loading level (stress) in the D-sys increases. Due to constant load characteristics, S_L varies linearly with λ . The real power observed at the substation is slightly less non-linear compared to the reactive power (Q_{SS}). At the initial loading of system, Q_{SS} is marginally below Q_L because the power at substation does not account for the capacitor bank injections.

The distribution system includes capacitors across various phases to provide reactive power support. By supplying reactive power locally, these capacitors improve the power factor and reduce the reactive power demand on the substation. As the λ increases, the Q_{SS} becomes increasingly non-linear due to rising losses within the D-sys. The typical variation of losses and power factor are depicted in Figure 3.5 and Figure 3.6, respectively.

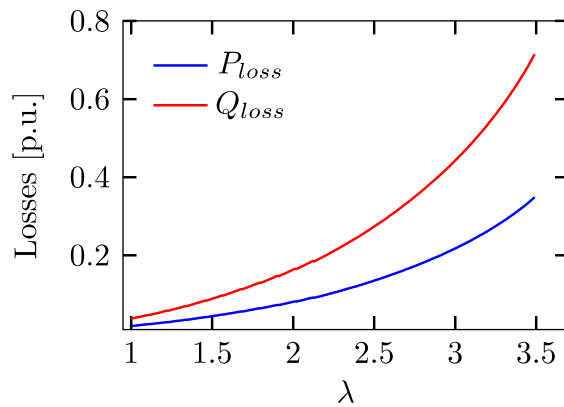


Figure 3.5 Variation of losses in distribution system.

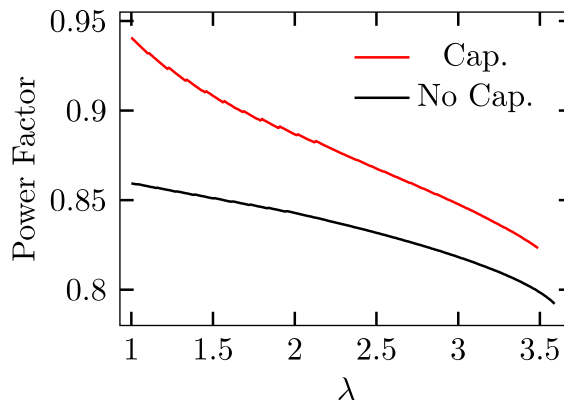


Figure 3.6 Variation of power factor at substation.

As the stress levels in the D-system rise, Q_{loss} increases non-linearly compared to P_{loss} , leading to a rapid reduction in the power factor at the substation. Figure 3.6 illustrates that incorporating capacitor banks into the D-system improves the power factor relative to systems without them. These banks provide essential reactive support, enhancing the system's response under varying load conditions.

Additionally, the impact of non-linearity can be observed through the tap positions of the D-system transformers, as shown in Figure 3.7. The D-system includes seven regulators, and the changes in tap position in response to system stress are unpredictable, varying from -16 to 16. This range reflects the number of tap changes per iteration in snapshot mode. Due to load increases, some regulators (Figure 3.7) may experience over-voltage conditions, prompting the tap position to step down to regulate the voltage. Conversely, the tap position of regulators may step up in response to under-voltage conditions. The increments and decrements of the tap positions depend on the configuration of the distribution network and cannot be generalized solely based on the overall load increase.

There is no generic way to explain about the non-linearity in the losses of the distribution network (Figure 3.5) as the system stress increases. One possible explanation is to interlink the tap positions of the regulators with the losses of the distribution network. Tap positions directly impact the voltage delivered in a distribution system, and changes in voltage affect the current flow and hence the system losses. As tap positions approach their maximum setting, the system may experience a significant increase in losses due to the higher current demand and potential inefficiencies in voltage regulation.

This part of the problem must be further explored to obtain clarity on impact of control actions and losses of the system related under different loading conditions of the system and to what extent these interactions impact at the T&D interfaces. One way to correlate the tap position with losses is by presuming that the non-linearity of the losses increases as more taps approach their maximum positions. This aspect of the problem must be further explored to elucidate the relationship between control actions and system losses under varying loading conditions. It is essential to understand the extent to which these interactions influence the T&D interfaces.

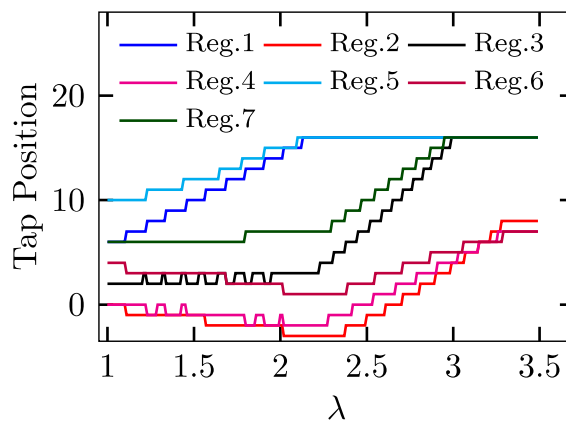


Figure 3.7 Tap positions inside D-sys.

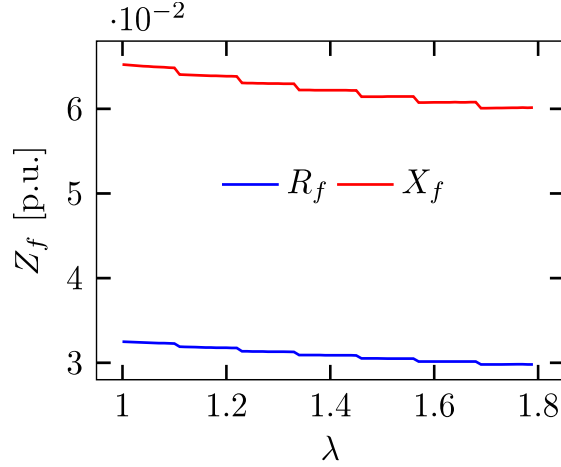


Figure 3.8 Variation of impedance at substation.

Figure 3.8 demonstrates the influence of λ on the equivalent impedance (Z_f) observed at the substation. With a constant substation voltage, increasing power levels result in a reduction of the equivalent feeder impedance perceived at the substation. By incorporating the equivalent feeder, we can achieve a more accurate representation of the aggregated model, as this approach accounts for the losses occurring within the D-system.

Increased stress scenarios significantly affect the D-system, making it essential to incorporate a full-scale distribution model for transfer capability studies. Load increases within the D-system introduce non-linearities in the power observed at the substation, which may not be adequately captured by traditional aggregated models used in stability analyses.

3.3.1 Impact of Load Models on Distribution System

Various load models are present within distribution networks, and the system's behavior is significantly influenced by the characteristics of the loads existing in the distribution system. Among these, the ZIP model is one of the most frequently encountered load models. The mathematical representation of the ZIP model is given by (3.2).

$$S = S_0 \left(c_z \left(\frac{V}{V_0} \right)^2 + c_i \left(\frac{V}{V_0} \right) + c_{pq} \right) \quad (3.2)$$

where V , P and Q are the voltage magnitude, real and reactive powers, respectively. V_0 , P_0 and Q_0 are the base voltage, base real power, and reactive powers. The coefficients c_z , c_i and c_{pq} correspond to impedance (Z), current (I) and power (PQ) loads, respectively.

From the equation, it is evident that the operating voltage of the system directly influences the power drawn by impedance and current loads. Conversely, PQ loads remain unaffected by changes in operating voltage. As the stress on the distribution network varies, the voltage at the load end fluctuates, resulting in changes in the power drawn by the loads based on their respective models.

The impact of load increments on the D-system is illustrated using the IEEE 123-node distribution system, which considers three distinct load models: constant Z, constant I, and constant PQ.

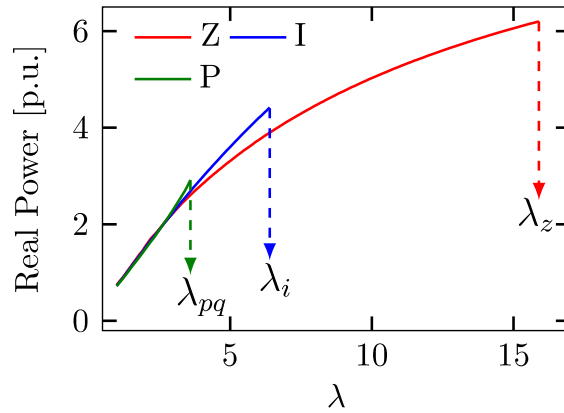


Figure 3.9 Real power seen at substation for different load models in D-sys.

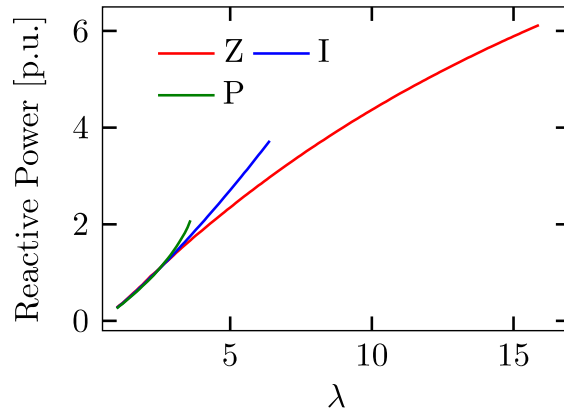


Figure 3.10 Reactive power seen at substation for different load models in D-sys.

The typical variation of S_{SS} as the loading level of the D-system increases is illustrated in Figure 3.9 and Figure 3.10. The load increment in the D-system is conducted at a constant substation voltage of 1 p.u., with all load models increased by the same λ (a 1% load increment is considered for this study). Both real and reactive power observed at the substation exhibit a non-linear relationship with respect to λ (maximum values), following the order $\lambda_z > \lambda_i > \lambda_{pq}$.

Constant PQ loads induce greater stress within the D-system. As the load increases and voltage levels decrease, the current drawn by constant PQ loads increases significantly, leading to higher losses in the system. This results in greater non-linearity in the power drawn at the substation, as depicted in Figure 3.10. Conversely, the voltage reduction associated with constant Z loads allows for a lower power draw at the same λ , which contributes to a higher loading margin compared to other load models.

Another perspective on the impact of stress in the D-system with different load models is provided by examining reactive power loss, as shown in Figure 3.11. The stress induced by constant PQ

loads leads to elevated reactive losses, even at lower load increments. This condition results in increased reactive power and a rapid decline in the power factor observed at the substation (illustrated in Figure 3.12). The decrease in power factor at higher load increments is notably less pronounced with constant Z loads, due to the reduced stress they exert.

It is also important to note that in this study, the load increment in the D-system is performed while maintaining the substation voltage at 1 p.u. A decrease in λ_z may occur if the substation voltage falls below 0.95 p.u..

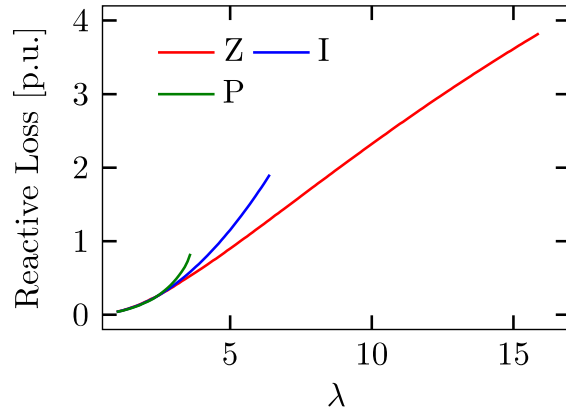


Figure 3.11 Reactive losses of D-sys.

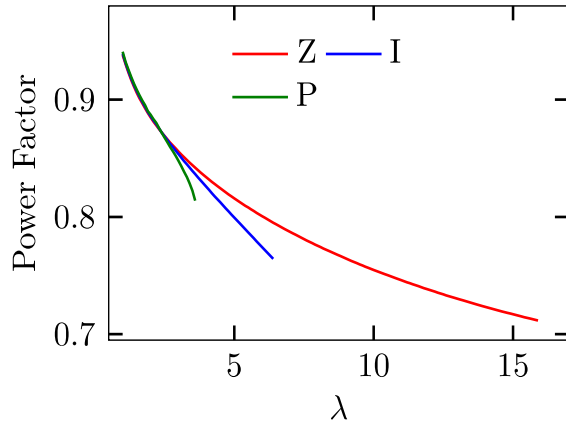


Figure 3.12 Power factor seen at substation.

To understand this impact, the load increment study on different load models within the D-system is evaluated across various substation voltages. λ_{max} obtained under these conditions is presented in Table 3.1.

An examination of Table 3.1 reveals that substation voltage significantly affects the loading level of the distribution network, with potential reductions at lower operating voltages.

Table 3.1 Impact of substation voltages on the load increment parameter

Substation Voltage (p.u.)	Max. λ_z	Max. λ_i	Max. λ_{pq}
1.05	20.52	7.05	4.00
1	16.72	6.53	3.65
0.95	13.20	6.00	3.28
0.9	9.97	5.46	2.95

Constant current and power loads exhibit similar ranges of λ_{max} compared to constant impedance load models. However, with constant impedance models, the loading factor decreases dramatically as the substation voltage declines. Therefore, it is essential to consider the types of loads present in the distribution network when conducting co-simulation studies.

3.4 Impact of Load Increment on Distribution Systems

DERs significantly influence system responses, with the extent of this impact largely determined by the level of DER power penetration and the configuration of the system. OpenDSS offers comprehensive modeling capabilities for solar photovoltaic (SPV) systems [33], enabling their integration across various loads and phases.

Typical specifications for SPV systems include power output, irradiance levels, temperature, efficiency, and power factor. The model operates on the assumption that the inverter can quickly identify the maximum power point (MPP), a simplification that has proven beneficial for interconnection studies. Additionally, OpenDSS's detailed modeling of SPV systems facilitates the simulation of various time-series data and snapshots. Below is an OpenDSS code snippet that specifies the SPV module for any distribution network [33]:

```
New PVSystem.PV_name phases= $N_p$  bus1=Bus_no kV=KV kVA=KVA irradiance= $N_{irr}$ 
~Pmpp= $P_{mpp}$  pf= $N_{pf}$ 
```

In this context, PV_name refers to the specified name for the photovoltaic system, N_p indicates the number of phases to which the SPV is connected, KV represents the voltage rating of the DER module, KVA denotes the rating of the SPV module, N_{irr} specifies the irradiance values, P_{mpp} indicates the maximum power point (MPP) power, and N_{pf} defines the power factor. This specification enables us to set the desired SPV power across different buses and phases of the distribution network, accommodating both balanced and unbalanced configurations.

The impact of SPV integration in the IEEE 123-node system with constant impedance loads is assessed at a substation voltage of 0.9 p.u., with a DER penetration level of 10% considered for analysis. The DERs are distributed across various nodes within the D-system. Figure 3.13 illustrates the typical real power observed at the substation as loading increases.

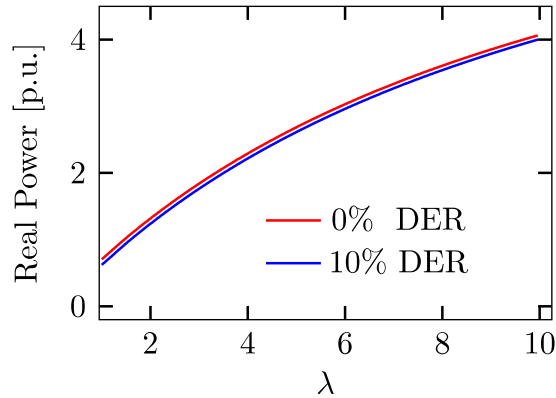


Figure 3.13 Variation of real power at substation in presence of DER.

An analysis of Figure 3.13 shows that the net power at the substation decreases due to the injection of power from the DERs, with this reduction directly related to the megawatts (MW) contributed by the DERs. At approximately 8 MW of power from the DER, only a slight reduction is noted at the initial load increment (i.e., $\lambda = 1$). Furthermore, the λ_{max} values across different DER scenarios appear to be comparable.

The SPVs are equipped with Smart Inverter Control (SInV), which enables the DERs to participate in voltage regulation within the distribution network. SInV facilitates Volt-Var Control (VVC), allowing SPVs to either inject or absorb reactive power. The typical VVC curve is illustrated in Figure 3.14. The injection (capacitive) or absorption (inductive) of VARs is determined by the voltage experienced at the SPV terminals and the available VAR support. This available VAR support is contingent upon the inverter rating and the maximum power point (MPP) power ($\sqrt{KVA^2 - P_{mpp}^2}$).

Two additional aspects of VVC are the droop and dead-band characteristics. The dead-band region, which typically ranges from 0.95 to 1.05 p.u., is characterized by zero reactive power, meaning that the DERs are not expected to participate in voltage regulation within this range. The droop characteristics define the controllable portion of the VVC, helping to ensure minimal reactive power variations in response to voltage fluctuations.

In OpenDSS, the VVC is specified as an XY curve by defining a variable number of points. Below is the code snippet for creating the XY curve in the OpenDSS script [33]:

```
New XYCurve.XY_curve npts=6 Yarray= (1.0,1.0,0,0,-1.0,-1.0)
~XArray= (0.5,0.9,0.95,1.05,1.15,1.5)
```

```
New InvControl.InvPVCtrl mode=VOLTVAR voltage_curve_ref=rated vvc_curve1=XY_curve
```

The npts parameter of the XY curve specifies the number of points on the VVC curve. The XArray and Yarray correspond to the voltage and available VARs of the VVC curve, as illustrated in Figure 3.14. The zero points in the Yarray indicate the dead-band of the VVC curve, while values of ± 1 represent the injection and absorption of VARs.

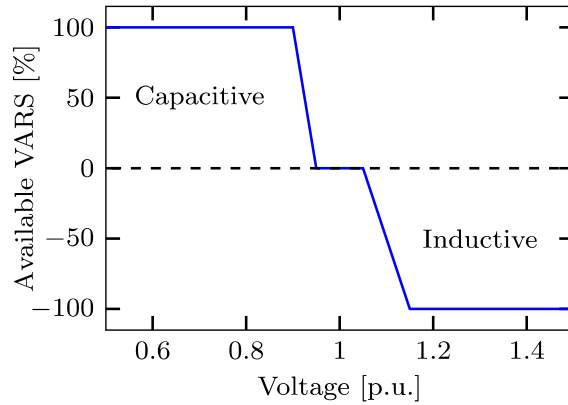


Figure 3.14 Typical VVC curve of SPV.

The SPVs are managed by the InvControl object in OpenDSS, with the mode set to VOLTVAR to regulate the reactive power output of the DERs. It is important to note that the VVC curve can be customized based on the operating scenario, which presents challenges when attempting to incorporate VVC into stability studies.

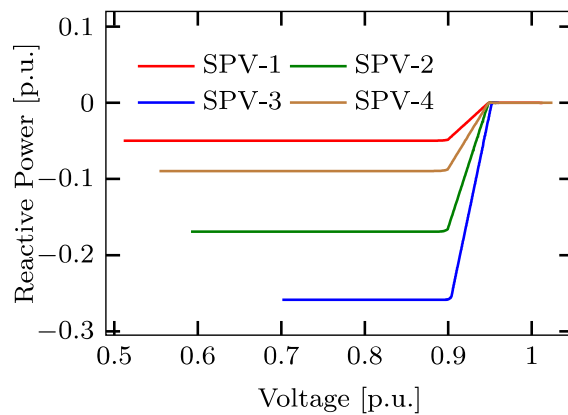


Figure 3.15 Variation of VAR power from DERs as a function of DER node voltage.

The typical VAR injection from the DERs under a 10% DER penetration scenario (for IEEE 123 node system) as a function of DER node voltage is illustrated in Figure 3.15. Within the voltage range of 0.95 to 1.05 p.u., the VAR support from the DERs is zero, indicating that the operating voltages are within the dead-band region.

When the node voltage at the SPVs falls below 0.9 p.u., the DERs begin to inject varying levels of reactive power, adhering to the droop characteristics of the VVC curve. Once the voltage drops below 0.9 p.u., the DERs inject maximum VAR into the distribution network, with the specific amount of VAR injection dependent on the ratings of the individual SPVs. For comprehensive VAR injection details, it is essential to have a complete understanding of the distribution system's footprint and associated data.

Table 3.2 Impact of VVC on the distribution system (Powers are expressed in p.u. with 100 MVA base)

% DER Penetration	S_{ss_0}	$S_{load_{max}}$	λ_{max}
0	$0.7 + j0.25$	$3.12 + j1.71$	9.97
10	$0.6 + j0.24$	$3.18 + j1.75$	9.98

The impact of VVC under a 10% DER penetration scenario is presented in Table 3.2. An examination of the table reveals that VVC does not significantly change the initial reactive power observed at the substation (S_{ss_0}). However, the real power at the substation decreases in relation to the power injections from the maximum power point (P_{mpp}).

The minimal variation in reactive power at the substation is attributed to the limited VAR injections from the DERs under nominal loading conditions. The values of $S_{load_{max}}$ across various DER scenarios indicate that the inclusion of VAR support within the distribution system only slightly enhances the load-handling capability. Consequently, one can anticipate a similar response in co-simulation studies.

A key aspect of this analysis is to highlight that the behavior of the distribution system is load-dependent and significantly influenced by substation voltages, as observed in T&D co-simulation studies. The effectiveness of VVC in distribution networks relies on the available VAR support, which can be comprehensively assessed through co-simulation. The challenge, however, lies in determining the extent to which VVC affects stability assessments within the distribution system.

3.5 T&D Co-simulation Framework for PV Analysis

The T&D framework for PV analysis effectively captures the transfer limits of the system by incorporating detailed modeling of the distribution system (D-system). Figure 3.1 and Figure 3.2 illustrate the co-simulation framework and the methodology for incrementing loads in the D-system, respectively. Additionally, Figure 3.17 presents a flowchart that outlines the T&D co-simulation framework used to generate the PV curves.

Initially, models are set up in both PSS/E and OpenDSS, with the substation voltage configured to $V_{B_{11}}$. The power flow is then solved in OpenDSS. For each simulation run, the power observed at the substation (S_{SS}), which represents the total of all three phases, is fed back to PSS/E at bus B_{11} . The load flow calculation is executed in PSS/E, and this iterative process continues until the voltage at distribution bus $V_{B_{11}}$ (as shown in Figure 3.1) remains less than 10^{-5} across successive iterations. The process is repeated till voltage at the distribution buses is less than 10^{-5} .

This tight coupling ensures accuracy in the voltages and powers obtained. The procedure is repeated for various load increments, terminating when power flow diverges in either system. As previously noted, the N_f factor is included to create loading conditions equivalent to those at the transmission level.

Within the co-simulation framework, individual loads in the distribution network are incremented, introducing stress to the system. Inclusion of N_f further intensifies this stress at the transmission level. This dual approach allows for an accurate assessment of power capability, as stress is effectively applied at both the transmission and distribution levels.

Another approach to performing PV curve analysis is by feeder increment (F-inc.), as shown in Figure 3.16. This method operates by gradually incrementing the net power at substation by $\Delta\lambda$. Specifically, for a given distribution network, the power at substation is scaled by N_f to meet the transmission loading level. The load power at the substation is then adjusted to $S'_{SS} = (N_f + \Delta\lambda)S_{SS}$. The co-simulation is performed with adjusted power (S'_{SS}), until the convergence criteria is satisfied.

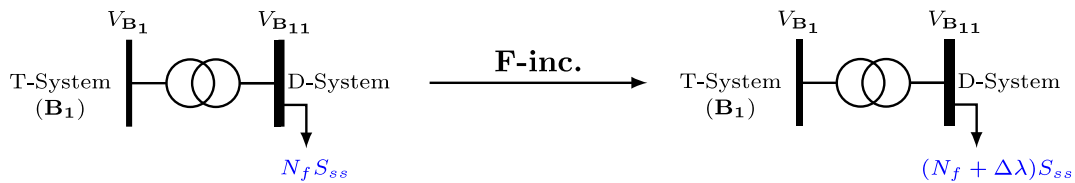


Figure 3.16 General schematic for feeder increment method.

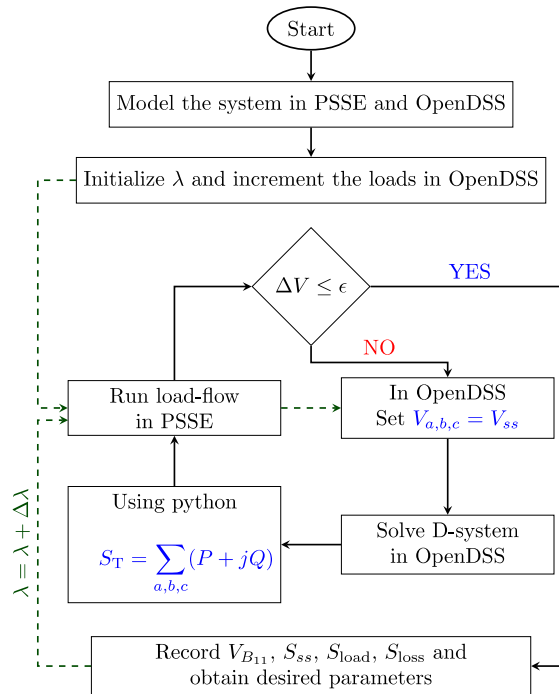


Figure 3.17 Flowchart illustration T&D co-simulation process for obtaining PV curves.

The loads within the D-system remain unchanged, meaning that this level of increment will primarily induce stress within the transmission system. As loading increases, the substation voltage varies, while the D-system is assessed at a fixed load but with fluctuating substation voltage. In

this study, we will focus our analysis on load increments within the distribution networks, as these increments can create stress at both the T&D systems.

3.6 Aggregated Model for PV Analysis

The aggregated model analysis necessitates the use of a single system solver, specifically a transmission solver. In this approach, the entire complex power network is modeled in PSS/E, with the corresponding distribution buses incorporated into this framework. Figure 3.18 illustrates the general schematic of the aggregated model, often referred to as the Agg. Model, which is utilized for conducting PV stability assessments.

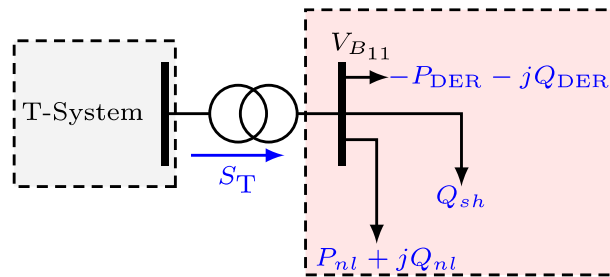


Figure 3.18 Aggregated model for stability studies.

A transformer with reactance X_T connects the low-voltage distribution buses to the high-voltage transmission buses. Aggregated models streamline stability assessments by omitting detailed representations of the distribution network. In these models, distribution system loads are represented as lumped constant power (PQ) loads.

S_{nl} denotes the total load and losses of the D-system under nominal loading conditions, while Q_{sh} represents the capacitance injections in the D-system, modeled as a negative reactive load for stability studies. In addition to the loads, aggregated models account for DER generation when assessing voltage stability. DER generation within the distribution network is represented as constant PQ injections ($P_{DER} + jQ_{DER}$) in the aggregated models. Here, P_{DER} reflects the real power generated by IBRs and remains constant across various operating conditions.

Conversely, the reactive support provided by IBRs is contingent upon the operating conditions of the D-system, making it challenging to directly translate its impact into aggregated models. In this work, we propose a methodology to replicate the VAR support from IBRs for voltage stability assessment, and we validate this approach across different operating scenarios.

3.6.1 Nominal Load Computation for Aggregated Models

For stability studies, the aggregated loads (S_{nl} , Q_{sh} , and P_{DER}) are estimated by analyzing the distribution network under nominal voltage conditions. A well-designed power network typically operates within a voltage range of 0.95 to 1.05 p.u., and under these conditions, the loads are expected to exhibit minimal sensitivity. However, due to varying load characteristics and imbalances within the D-system, significant variations may occur under different operating scenarios.

It is important to note that N_f is considered in determining the load parameters for aggregated models (with N_f used to scale the powers to meet the transmission loading level). The two different approaches to obtain the nominal loading of the D-sys are outlined as follows.

1. To evaluate the D-system, select a substation voltage range of 1 to 1.05 p.u. and utilize OpenDSS to compute the total load and losses (S_{nl}), total capacitance injections (Q_{sh}), and DER generations (P_{DER}). While this method for computing nominal load can be effective, it may become inefficient if the voltage within the D-system drops below the specified operating range. Such a situation could result in higher nominal load estimates, particularly if the distribution network comprises a mix of load models.
2. The most efficient method for representing the nominal loading of the D-system for stability studies is to conduct a T&D co-simulation. The schematic representation of this approach is illustrated in Figure 3.19. In this setup, a low-voltage distribution bus (B_{11}) is connected to a transmission bus (B_1) via a transformer. The T&D co-simulation is carried out between PSS/E and OpenDSS by exchanging the bus voltage ($V_{B_{11}}$) and the power from the substation (S_{ss}). Once the load flow converges, the corresponding loads, capacitive injections, and DER powers (if applicable) are derived from the co-simulation data, ensuring that the obtained parameters satisfy (3.3).

$$S_{ss} = S_{nl} + S_{sh} + S_{DER} \quad (3.3)$$

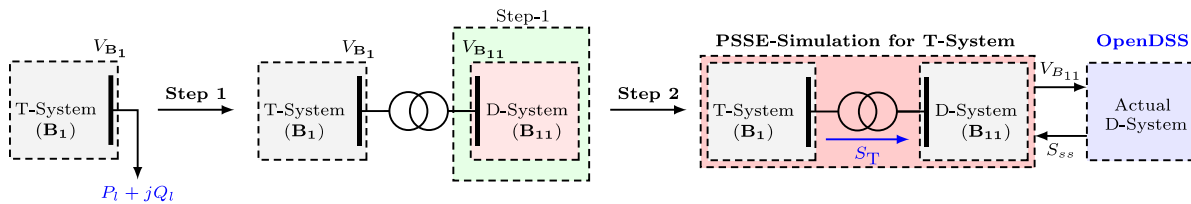


Figure 3.19 Step by step procedure to obtain nominal loading of aggregated model.

This method for obtaining nominal loading incorporates detailed modeling of the D-system, accurately reflecting the effective loads and DER injections. It is important to note that the co-simulation framework is utilized solely to derive the nominal loading of the D-system; the remainder of the stability assessment is conducted using the aggregated model depicted in Figure 3.19. The PV curve with the aggregated model is generated similarly to the T&D co-simulation, involving incremental adjustments to the loads. In this scenario, both real and reactive loads are incremented by λ , while shunt injections and DER powers remain constant throughout the PV stability assessment. The governing equation for load increment is given in (3.4).

$$S'_{nl} = S_{nl}(1 + \lambda) \ \& \ Q_{sh} = Q_{sh} \quad (3.4)$$

In most stability studies, DERs are modeled as unity power factor DER sources, with P_{DER} represented as a negative load (where $Q_{DER} = 0$), thereby excluding any reactive power support from the IBRs.

However, incorporating VAR support from IBRs is crucial, as it significantly affects the system's transfer capability and alters the overall system response.

3.6.2 Incorporation of VVC into Aggregated Models

In most stability studies, DERs are modeled as unity power factor sources, with P_{DER} represented as a negative load (where $Q_{DER} = 0$), thereby excluding any reactive power support from the IBRs. However, incorporating VAR support from IBRs is crucial, as it significantly affects the system's transfer capability and alters the overall system response. To address this, we define two aggregated models: Agg.Model without VVC and Agg.Model with VVC, as illustrated in Figure 3.20 and Figure 3.21, respectively.

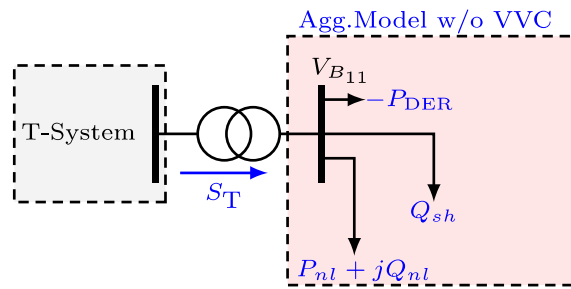


Figure 3.20 Aggregated model at UPF mode.

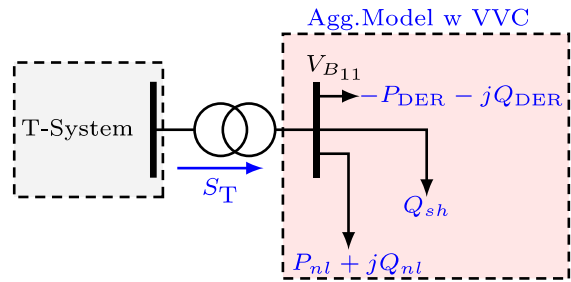


Figure 3.21 Aggregated model with VAR support (Agg.Model w VVC).

The total net load seen at the D-sys bus by Agg.Model w/o VVC is given by (3.5).

$$S'_{nl} = P_{nl} - P_{DER} + j(Q_{nl} - Q_{sh}) \quad (3.5)$$

In this model, the net real load observed on the D-system bus is reduced. Conversely, the effective load on the bus when using the Agg.Model with VVC is described by Eq. 6.

$$S'_{nl} = P_{nl} - P_{DER} + j(Q_{nl} - Q_{sh} - Q_{DER}) \quad (3.6)$$

In the Agg. Model with VVC, both the real net load and the net reactive power at the D-system bus are modified, resulting in an expected increase in voltage levels. This raises a critical challenge: how to accurately model the VAR support without utilizing a detailed representation of the D-system.

Within the T&D co-simulation framework, the detailed modeling provides insight into how VAR support directly impacts the power observed at the substation. To address this for the Agg.Model with VVC, we have developed a lookup table approach that translates the VAR support provided by IBRs. This methodology can be seamlessly implemented in a Python environment, allowing for efficient integration into stability assessments and enhancing the overall accuracy of the model.

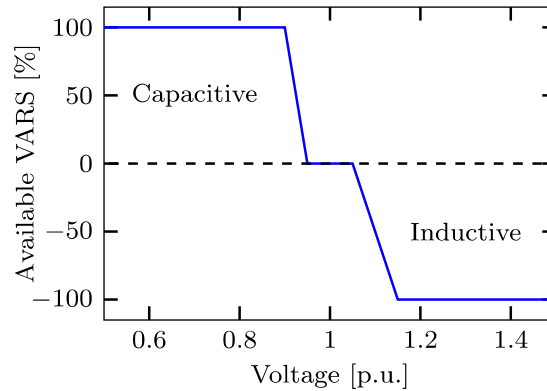


Figure 3.22 Typical VVC curve of DER.

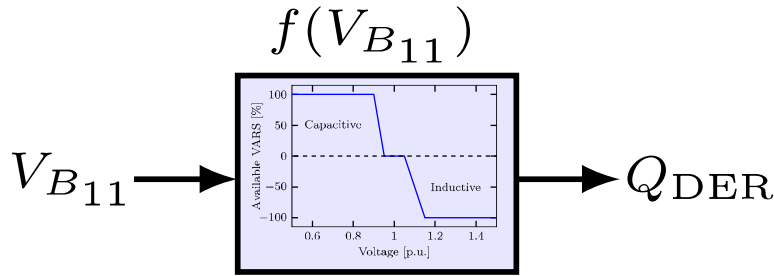


Figure 3.23 Lookup table approach to mimic VVC.

Figure 3.23 illustrates the core concept behind the developed methodology. The typical VVC, depicted in Figure 3.22, shows the available VAR support, which can be calculated for a single DER using (3.7).

$$KVAR = \sqrt{(KVA)^2 - (KW)^2} \quad (3.7)$$

where KVA represents the total rating of the inverter and KW indicates the maximum power point (MPP) power available from the solar panel. For a system comprising n DER modules in the D-

system, the total available VAR support is expressed as: i.e., $KVAR_{net} = KVAR_1 + KVAR_2 + \dots + KVAR_n$.

In the lookup table approach, the x-axis of the curve corresponds to the voltage on the VVC curve, while the y-axis represents the maximum VAR support available ($\pm Q_{DER} = \pm KVAR_{net}$). The reactive power (Q_{DER}) in the aggregated model varies based on the voltage at bus B₁₁, such that: $Q_{DER} = f(V_{B_{11}})$.

This relationship ensures a variable reactive power support from the DERs. This approach effectively captures the impact of VVC, as the VAR support from IBRs is influenced by voltage levels within the distribution network. However, it is important to note that the VAR injection is contingent upon the voltage experienced by the DER buses within the D-system.

Consequently, one can expect an increase in voltage due to this methodology, as Q_{DER} is dependent on the interface voltage and does not rely on a detailed model of the D-system. The available DERs and their respective ratings, along with the VVC curves, can be easily extracted from OpenDSS using a Python interface. The lookup table is constructed using the data from the VVC curve, with the y-axis set to Q_{DER} , facilitated by the *SciPy* module.

Algorithm 1 Framework for translating the VVC impact to PSS/E.

```

1: Read data for study
2: Initialize the PSS/E using the *.raw file and add distribution bus (B11) via transformer
3: Add D-sys bus at desired transmission bus. Obtain the nominal loading of aggregated model
and initialize  $\lambda$  and set CNF = True (CNF is convergence flag)
4: for  $\lambda \leftarrow \text{max to min}$  do
5:     Increment  $S_{nl}$  by  $\lambda$  and run the power flow
6:     while CNF is True do
7:         Obtain  $V_{B_{11}}$  and set  $Q_{DER} = f(V_{B_{11}})$  and run the power flow in PSS/E
8:         if  $\Delta V_{B_{11}} \leq \epsilon$ 
9:             break
10:        else
11:            Set  $Q_{DER} = f(V_{B_{11}})$  and run the power flow in PSS/E
12:        end if
14:        if CNF == False
15:            break
16:        end if
18:    end while
19:    Record  $V_{B_1}$ ,  $V_{B_{11}}$ ,  $Q_{DER}$  and  $S_T$ 
20: end for

```

The implementation of the lookup table approach for VVC is detailed in Algorithm-1. Once the model is initialized in PSS/E and the nominal loading for the aggregated models is determined, an initial load flow analysis is conducted in PSS/E. Utilizing the voltage at bus B₁₁ ($V_{B_{11}}$), the reactive

power Q_{DER} is fixed and iteratively adjusted until the voltage at the bus drops below a threshold of 10^{-5} . These internal iterations facilitate smoother reactive power injections at the bus.

However, it is important to acknowledge that this VVC incorporation represents an oversimplified model. In real-world scenarios, there may be instances where IBRs do not fully participate in providing VAR support, potentially leading to discrepancies between the modeled and actual system behavior.

4. Results and Discussions

The objective of the section is to provide concrete analysis on to what extent does the T&D co-simulation studies are comparable with that of aggregated model for stability studies under high IBR penetration.

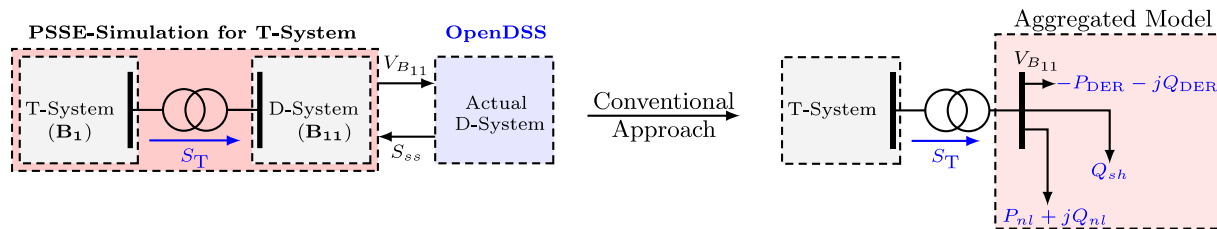


Figure 4.1 Framework for comparison of co-simulation studies and aggregated models.

The framework for comparing different models is illustrated in Figure 4.1. Our primary objective is to analyze how voltage in the distribution system (D-sys) fluctuates as power demand increases across the transmission and distribution (T&D) interface. To facilitate this analysis, we modify the loads within the D-sys during co-simulation studies using a scaling factor (λ), while maintaining constant capacitance and distributed energy resource (DER) injections in the distribution network. Simultaneously, the apparent power (S_{nl}) of the aggregated models is increased by the same parameter (λ), without altering the reactive power (Q_{sh}) or the contributions from DERs (S_{DER}).

The simulations include a range of transmission systems, including the IEEE 9-bus system [34], the 240 WECC system [35], and a confidential System-X (large real system in the Eastern interconnection, the details of which are protected under a non-disclosure agreement).

Table 4.1 Distribution systems connected to transmission buses for stability assessment

Transmission System	Number of distribution systems connected
IEEE 9-bus system	1
240 WECC system	1
System-X	20

Table 4.1 illustrates the number of distribution systems connected to the transmission network for the PV curve analysis. While we analyze multiple buses from the IEEE 9-bus and 240 WECC systems, our focus is on scenarios where a single distribution network connects to the transmission system. In the case of System-X, twenty load buses in a specific zone are replaced with the distribution network for stability assessment. For the test cases, the loading level of each transmission bus is matched using a feeder multiplication factor (N_f).

It is important to note that distribution systems are not inherently designed for stability studies. They are primarily engineered to accommodate expected average load demands, focusing on reliability and efficiency under typical conditions. As a result, these networks may not adequately

address the increasing load demands encountered during stability assessments. To effectively manage these varying loading capabilities, we strengthen the distribution networks, reinforcing their capacity to support thorough stability assessments. This proactive approach allows us to account for unexpected fluctuations and maintain system stability under diverse operational conditions. Further details regarding the strengthening of the distribution network can be found in Appendix B.

While our analysis encompasses various distribution networks, including the IEEE 13-node, 8500-node, and 9500-node systems, we will primarily focus on the modified IEEE 123-node distribution network. In this network, DERs are strategically allocated across distinct phases and loads, with VVC enabled by default. Additionally, we will evaluate the impact of different penetration levels of IBRs with VVC on the transfer capability margin, utilizing a co-simulation framework and aggregated models.

4.1 Analysis of IEEE 9-bus and IEEE 123 Node Distribution System

We begin by presenting the PV analysis for the IEEE 9 Bus-123 Node distribution network, with the distribution system (D-sys) connected to bus seven of the transmission system. The D-sys is enhanced by reducing the line impedance by a factor of five and halving the nominal loads. Additionally, the distribution network is assumed to have constant impedance loads.

Figure 4.2 displays the typical PV curve obtained at the low-voltage bus (B_{11}) and illustrates how varying the x-axis can shift the perspective of the analysis. The figure compares the PV curves generated using two methodologies, with λ as the x-axis. It shows that the co-simulation method exhibits higher loadability compared to the aggregated model. This observation is attributable to the constant impedance loads within the D-sys, whose characteristics are influenced by voltage levels. The net power observed at the substation fully accounts for the characteristics of the D-sys under co-simulation. Representing the net substation power as a PQ load model within the T&D co-simulation framework is sufficient to capture the dynamics of the distribution network effectively.

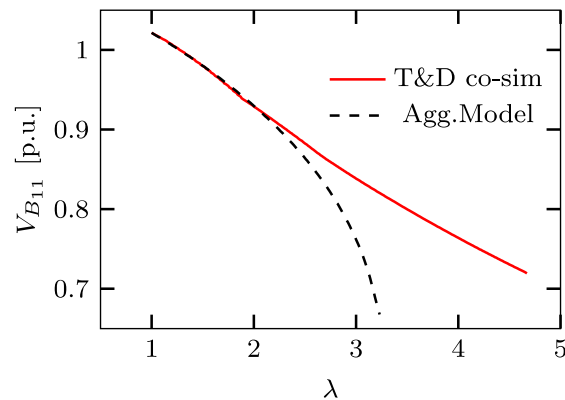


Figure 4.2 PV curve with respect to λ as x-axis.

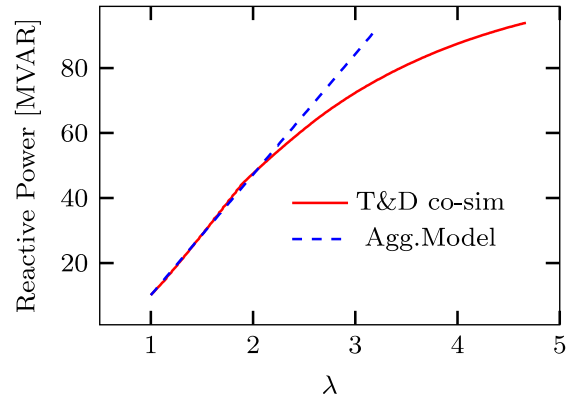


Figure 4.3 Variation of reactive power with respect to λ as x-axis.

The variation of power seen at substation is shown in Figure 4.3 and shows that the aggregated models have higher reactive power for lower load increments when compared with that of co-simulation. As a result, the aggregated models reach the nose point earlier (with λ plotted on the x-axis), which may hinder their ability to accurately reflect power transfer capabilities across the T&D interface.

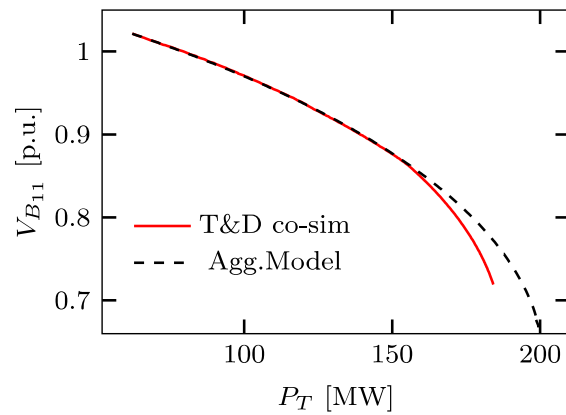


Figure 4.4 PV curve with respect to P_T as x-axis.

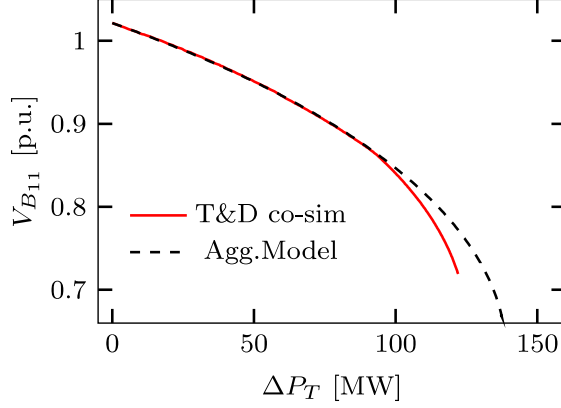


Figure 4.5 PV curve with respect to ΔP_T as x-axis.

The precise transferability can be analyzed with respect to P_T as the x-axis, as illustrated in Figure 4.4. This comparison shows that the aggregated model (198 MW) presents an overestimated margin relative to the T&D co-simulation (183 MW). An alternative method for plotting the PV curve is to use incremental transfer (ΔP_T) as the x-axis, as defined by (4.1).

$$\Delta P_T = \sum_{k=1}^{N_d} P_{T_k} - P_{T_0} \quad (4.1)$$

where N_d is the number of distribution networks connected to transmission grid, and P_{T_0} is the initial power transfer across the T&D interface. While using ΔP_T as x-axis, the PV curves begin at zero and effectively illustrate the transferability margin achieved with different models. Figure 4.5 displays a typical PV curve with ΔP_T as the x-axis, indicating that the aggregated model shows a higher margin compared to the T&D co-simulation. This discrepancy arises primarily because aggregated models do not account for any losses occurring within the distribution network.

4.1.1 Impact of DER on Stability Assessment

The impact of DER is assessed by examining various levels of penetration within the IEEE 123-node system. In this configuration, DERs are distributed across different loads and phases of the distribution network, with the VVC feature enabled. When VVC is active, the DERs are assumed to deliver 100% of the available reactive power (VARs). Table 4.2 outlines the DER capabilities considered for the stability assessment, with DER percentages expressed based on the nominal loading of the distribution network.

The integration of DER affects the power flow across the transmission and distribution (T&D) interface, depending on the level of real power penetration from the DER. The PV curves under various DER scenarios, obtained through co-simulation without VVC enabled, are presented in Figure 4.6 and Figure 4.7, with P_T and ΔP_T as the x-axes respectively.

Table 4.2 DER capabilities considered for analysis of IEEE 9-bus and IEEE 123 node distribution system

% DER Penetration	P_{DER} (MW)
0	-
10	6
25	15
40	25

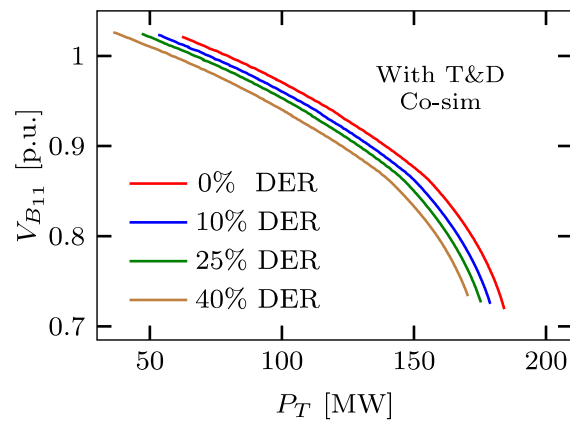


Figure 4.6 PV curve with respect to P_T as x-axis under DER penetrations.

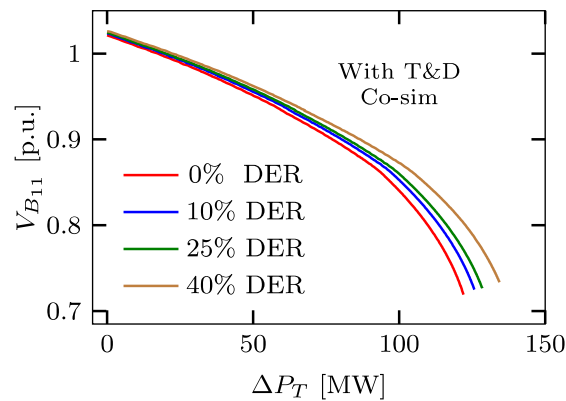


Figure 4.7 PV curve with respect to ΔP_T as x-axis under DER penetrations.

As DER penetration increases, the net load perceived by the transmission system also rises, causing the curves to shift left, as illustrated in Figure 4.6, and leading to a decrease in the maximum P_T . The inclusion of DER enhances the power transfer capability, as shown in Figure 4.7, which is directly influenced by the level of power penetration.

Moreover, the presence of DER in the distribution network results in a reduction of the power observed at the substation. Consequently, the initial voltage of the PV curve increases with rising DER penetration. Table 4.3 demonstrates how DER inclusion modifies the initial power seen at the substation, as derived from the co-simulation results. Notably, the data in Table 4.3 reveals that while the real power at the substation significantly decreases, the reactive power remains largely unchanged as DER penetration increases.

Table 4.3 Impact of DER penetration at the T&D interface

% DER Penetration	P_{DER} (MW)	P_T (MW)	Q_T (MVAR)
0	-	62	10.1
10	6	56	10.0
25	15	47	9.8
40	25	36	9.6

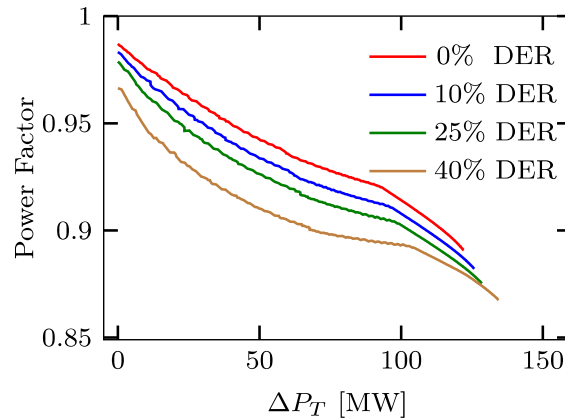


Figure 4.8 Variation of power factor seen at substation.

The real power observed at the T&D interface decreases significantly, leading to a rapid reduction in the power factor at the T&D interconnection, as illustrated in Figure 4.8, under conditions of higher DER proliferation. The total load managed by the distribution network, calculated at the nose point of the PV curve, is presented in Table 4.4. The loads identified through the co-simulation reflect the effective loads seen by the constant impedance loads, indicating that the integration of generation within the distribution network influences its load-handling capability to some extent.

The maximum ΔP_T across various DER scenarios, as shown in Table 4.4, reveals no direct correlation with DER capability, suggesting that the limits are dependent on the dynamics of both T&D systems. Furthermore, it is crucial to note that increased DER penetration does not significantly enhance the power transferability of the T&D systems.

Figure 4.9 presents a comparison between the co-simulation and aggregated models, using ΔP_T as the x-axis, under various DER penetration levels. The aggregated model employed for this analysis is the aggregated model without VVC, meaning that Q_{DER} is set to zero. The P_{DER} capabilities, as detailed in Table 4.5, are treated as negative loads within the aggregated model, as shown in Figure 4.1. An examination of the PV curve reveals that the aggregated models yield a higher margin. This outcome is anticipated, as these models do not account for losses, leading to more optimistic results.

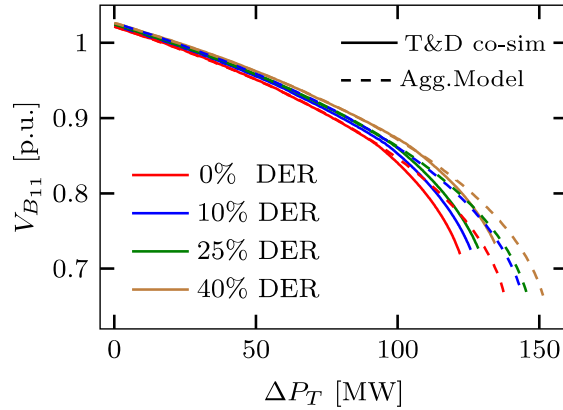


Figure 4.9 PV curve with respect to ΔP_T as x-axis under DER penetrations.

Table 4.4 Maximum load handled in distribution network under co-simulation

% DER Penetration	P_{DER} (MW)	P_{Load} (MW)	ΔP_T (MW)
0	-	180	122
10	6	181	124
25	15	185	129
40	25	188	136

Table 4.5 Incremental transfer power [in MW] under different DER scenarios

% DER Penetration	T&D co-simulation	Aggregated Model
0	122	134
10	124 (+2)	140 (+6)
25	129 (+7)	145 (+11)
40	136 (+14)	151 (+21)

Table 4.5 presents the maximum ΔP_T obtained using various models, clearly indicating that the aggregated models exhibit an increase in transferability margin as DER penetration rises. However, this margin increment does not follow a fixed trend; it cannot be generalized that a specific amount of DER will consistently yield the same increase in transfer limit.

The values in parentheses in Table 4.5 indicate the change in transfer limit from the base case, which is the no DER scenario. As the percentage penetration increases, the maximum transfer limit in the T&D co-simulation rises by 14 MW. In contrast, the aggregated model shows an increment of 21 MW for the same 40% DER penetration. This suggests that one can estimate the transfer limit with the aggregated models based on the DER capability of the distribution network.

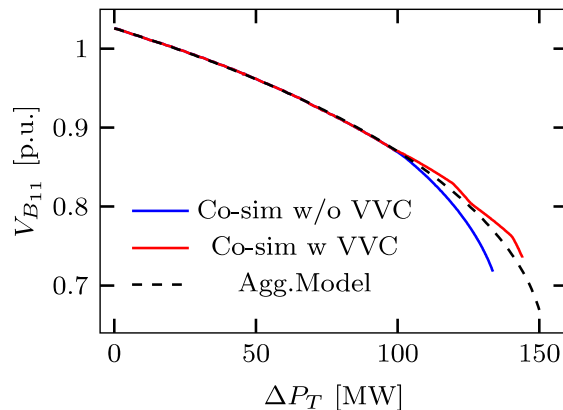


Figure 4.10 PV curve for IEEE 9 Bus-123 Node system with VVC enabled.

Table 4.6 Maximum incremental transfer obtained with different models

Model	Max. ΔP_T [MW]
T&D co-sim w/o VVC	134
T&D co-sim w VVC	144
Aggregated Model	150

The impact of VVC on transferability is illustrated in Figure 4.10 for the 40% DER scenario, where $P_{DER} = 23$ MW. The same distribution network is evaluated both with and without VVC to highlight its influence on the transferability limit. The aggregated model used in this study assumes $Q_{DER} = 0$, representing the aggregated model without VVC. Comparisons with co-simulation studies reveal that the inclusion of VVC enhances the transfer limit to some extent compared to the model without VVC. The maximum incremental transfers obtained in this analysis are presented in Table 4.6.

The reactive support provided by VVC contributes an additional 10 MW increment, which is influenced by the level of VAR support from the IBRs. The aggregated model demonstrates a close match even in the absence of reactive modeling. Furthermore, the initial point of the PV curve

aligns well because the operating voltage of the substation (1.02 p.u.) falls within the dead-band region of the VVC (with $Q_{DER} = 0$). As a result, the aggregated model offers a reasonable response for estimating transfer limits. Moving forward, we will focus on how the incremental transfer of the system is affected by varying levels of DER penetration.

4.2 Analysis of IEEE 240 WECC and IEEE 123 Node Distribution System

The assessment of the PV curve for the 240 WECC system at Bus 6401 [35] is conducted by evaluating various DER scenarios. The zoomed portion of Bus 6401 is shown in Figure 4.11. This system comprises four areas and multiple generation sources, including photovoltaic (PV), wind, and synchronous generators. While the analysis encompasses various buses within the 240 WECC system, this assessment will specifically focus on the stability evaluation when the distribution network is connected to Bus 6401.

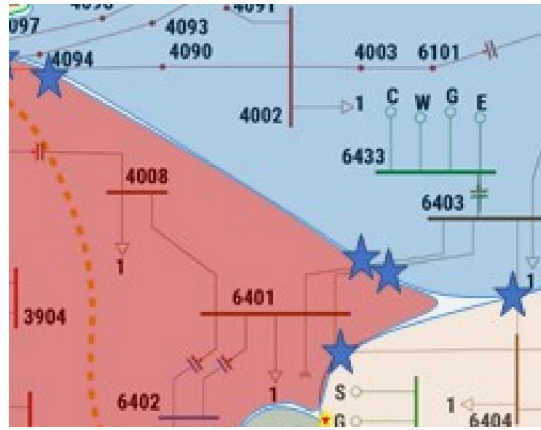


Figure 4.11 Detailed view of Bus 6401 within the 240 WECC System [35].

For this analysis, the IEEE 123-node distribution network serves as the framework, allowing for a realistic representation of operational conditions. To create this scenario, the loading of the distribution system (D-sys) is intentionally reduced to one-fifth of its nominal capacity, while the line impedances remain unchanged. Additionally, the distribution power is scaled by a factor of 100 ($N_f = 100$) to align with the nominal loading requirements of the transmission network. Various DERs with VVC capabilities are strategically distributed across different load levels within the D-sys, enhancing the assessment's comprehensiveness.

Table 4.7 DER capabilities considered for stability study of 240 WECC – IEEE 123 node system

% DER Penetration	P_{DER} (MW)	Q_{DER} (MVAR)
10	17	± 10
25	45	± 23
40	84	± 44

Table 4.7 outlines the capabilities of the DERs included in the analysis, with DER penetration defined in relation to the nominal loading of the distribution system (D-sys).

The typical PV curve generated under various DER scenarios is illustrated in Figure 4.12, highlighting the different models' estimates of the transfer limit. This study focuses on two distinct aggregated models: the Agg.Model w/o VVC (Agg w/o VVC) and the Agg.Model with VVC (Agg w VVC).

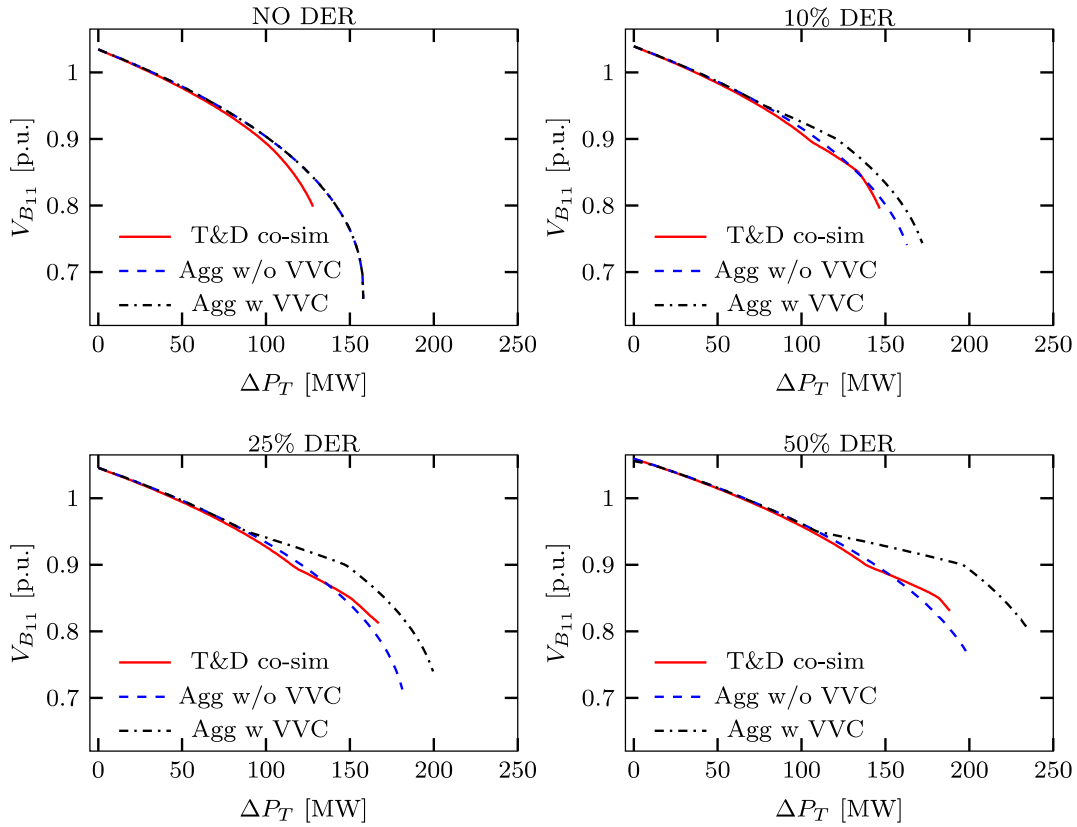


Figure 4.12 PV curve obtained for 240 WECC under different DER penetration scenarios.

In these models, the P_{DER} remains constant and is determined by the level of DER penetration. For the Agg w/o VVC model, the Q_{DER} is fixed at zero, remaining unaffected by changes in the voltage at the distribution system bus. In contrast, the Q_{DER} for the Agg w VVC model adjusts in response to the voltage observed at the distribution system bus. Across all models, it is evident that as DER penetration increases, the incremental transfer power rises, resulting in a decrease in the net power perceived by the transmission network.

In the absence of DER penetration, aggregated models (with and without VVC) exhibit similar responses. Table 4.8 presents the maximum ΔP_T across various DER penetration levels. The transfer limit increases with the rise in reactive power support from IBRs, and the co-simulation effectively captures this margin through its comprehensive modeling of the distribution network.

Table 4.8 Incremental transfer power [in MW] under different DER penetration.

% DER Penetration	T&D co-simulation	Agg.Model w/o VVC	Agg.Model w VVC
0	128	158	158
10	145	162	171
25	167	181	197
40	188	204	233

For the Agg.Model without VVC, the transfer margin obtained aligns closely with the estimates derived from co-simulation. In contrast, the Agg.Model with VVC tends to overestimate the transfer margin, primarily due to its approach of injecting reactive power based on the D-sys voltage. This model does not accurately reflect the actual reactive power contribution from the IBRs, as the reactive power injection is based on the voltage at the substation. This oversimplification leads to an inflated margin in the models with VVC.

A critical insight from this analysis is that the aggregated model without VVC may be sufficient for estimating the transfer limit, even under higher levels of DER penetration. This finding underscores the importance of model selection in accurately assessing transfer capabilities in distribution networks.

4.3 Analysis of System X and IEEE 123 Node Distribution System

System X is a complex network comprising numerous interconnections, areas, and zones. The transferability analysis of this system focuses on both sinks (loads) and sources (generators). An incremental study is conducted by systematically increasing the loads within the zone, with corresponding increases in MW generation. Generator increments occur only if the maximum generation limit exceeds the current set point. Should this limit be reached, any necessary MW increments are managed by slack buses.

Table 4.9 DER capabilities consider for stability study of System X and IEEE 123 node system

% DER Penetration	P_{DER} (MW)	Q_{DER} (MVAR)
25	241	± 127
50	473	± 263

For this analysis, the IEEE 123 node distribution system is evaluated under scenarios with 0%, 25%, and 50% DER penetration. Three distinct case studies are performed, each utilizing different load models: constant impedance, constant current, and constant power loads, to assess the transfer limits under varying DER conditions. To provide a realistic baseline for the no-DER scenario, the

nominal load of the D-sys is reduced by a factor of 10, while the line impedances remain unchanged.

Table 4.9 presents the DER capabilities considered for this study, with the P_{DER} indicated at nominal loading of the D-sys. Aggregated models, both with and without VVC, are utilized to estimate the system's transfer margin. is defined at 990 MW and 275 MVAR, with simultaneous increments applied across all loads.

For analytical purposes, we focus on plots related to the bus experiencing the minimum voltage. Initially, the assessment will be conducted using the constant impedance load model to evaluate system stability.

4.3.1 Results for Constant Impedance Loads

The behavior of constant impedance loads is influenced by the node voltage within the distribution network. The typical PV curves generated under this scenario, specifically at 50% DER penetration, are illustrated in Figure 4.13 and Figure 4.14.

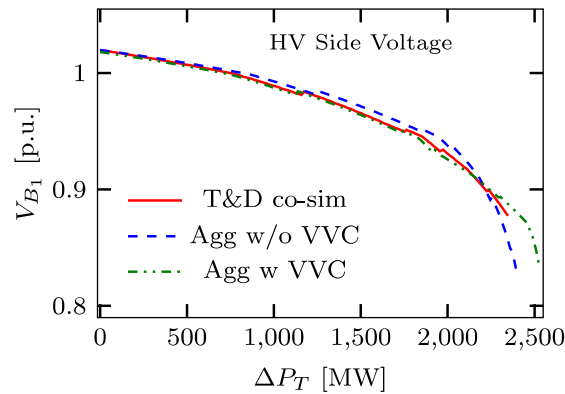


Figure 4.13 HV side voltage for 50% DER scenario.

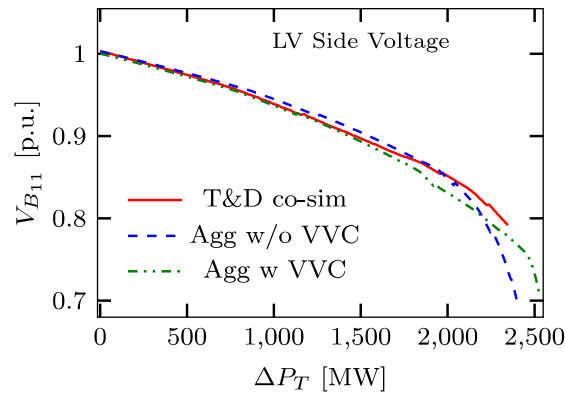


Figure 4.14 LV side voltage for 50% DER scenario.

The high-voltage (HV) side voltage, represented as V_{B_1} in Figure 4.13, shows that the aggregated model with VVC aligns well with the T&D co-simulation for voltages up to the 0.9 p.u. range, both in terms of transfer limits and voltage estimates. Meanwhile, the low-voltage (LV) side voltage depicted in Figure 4.14 indicates that the inclusion of VAR support in the aggregated models yields more accurate voltage estimates when levels are above 0.9 p.u. However, this approach can lead to overestimated margins due to excessive reactive power injections at lower voltage levels.

Table 4.10 Max. ΔP_T [in MW] from different studies with constant impedance loads

Type of Study	No DER		25% DER		50% DER	
	P_{T_o}	Max P_T	P_{T_o}	Max P_T	P_{T_o}	Max ΔP_T
T&D co-sim	964	1934	723	2135	490	2347
Agg.Model w/o VVC	964	1957	723	2131	490	2398
Agg.Model w VVC	-	-	723	2237	490	2524

Table 4.10 presents the maximum ΔP_T for constant impedance loads in the distribution system under various DER penetration levels. P_{T_o} at the D-sys bus decreases as DER capabilities increase, resulting in enhanced system transferability. The aggregated model without VVC demonstrates a strong alignment with T&D co-simulation results, with the estimated margin being either low or high but generally within a reasonable range of the true margin. In contrast, the aggregated model with VVC tends to provide an overestimated margin, largely due to the oversimplification of VAR support representation in these aggregated models.

4.3.2 Results for Constant Current Loads

In this scenario, the distribution network is modeled with constant current loads, which are anticipated to impose greater stress compared to constant impedance loads. Observations from the D-sys indicate that constant impedance loads tend to reach their loadability limits at lower load increments, primarily due to a rapid decline in substation voltage at the T&D interface. Consequently, one can expect a higher incremental margin with constant current loads.

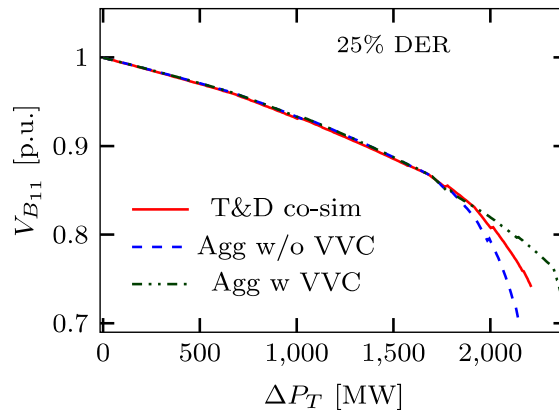


Figure 4.15 LV side voltage for 25% DER scenario.

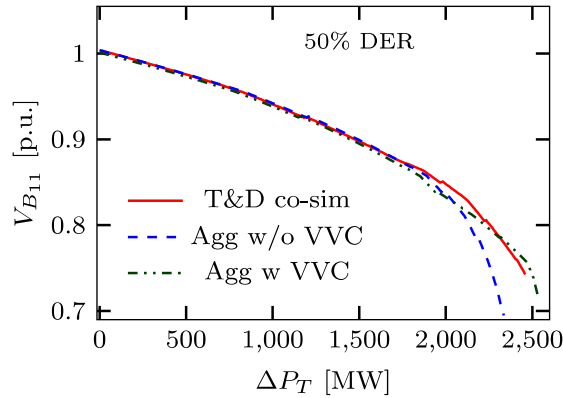


Figure 4.16 LV side voltage for 50% DER scenario.

Table 4.11 Max. ΔP_T [in MW] from different studies with constant current loads

Type of Study	No DER		25% DER		50% DER	
	P_{T_o}	Max P_T	P_{T_o}	Max P_T	P_{T_o}	Max ΔP_T
T&D co-sim	950	1967	707	2211	478	2459
Agg.Model w/o VVC	950	1966	707	2144	478	2335
Agg.Model w VVC	-	-	707	2374	478	2535

The typical PV curve seen at LV side of a bus under 25% and 50% DER penetrations are shown in Figure 4.15 and Figure 4.16, respectively. Under both scenarios, it is observed that the aggregated model without VVC underestimates the transfer margin when compared to the T&D co-simulation results. This deviation becomes more pronounced as DER penetration increases.

Table 4.11 demonstrates the maximum incremental transfer, indicating that the transfer capability limit of T&D systems rises with higher DER penetration. In the no DER scenario, P_{T_o} is lower than that of the constant impedance loads, and the aggregated model without VVC provides an underestimated margin for this situation. Conversely, the trend of overestimated margins with the aggregated model with VVC remains consistent across all DER scenarios. The inclusion of VVC produces a reasonable match with T&D co-simulation for voltage levels ranging from 0.95 to 1.05 p.u., and it aligns more closely with the nose point voltage compared to the aggregated model without VVC.

4.3.3 Results for Constant Power Loads

Constant power loads exert more stress on the network compared to other load models. In this scenario, the distribution system (D-sys) is composed of constant power loads, and the typical PV curves at the high voltage (HV) side under various DER scenarios are illustrated in Figure 4.17 and Figure 4.18, respectively. The aggregated model without VVC demonstrates a strong correlation with observed performance, even at higher DER penetrations. This alignment occurs

because the constant PQ load model representation creates stress levels comparable to those seen in T&D co-simulation.

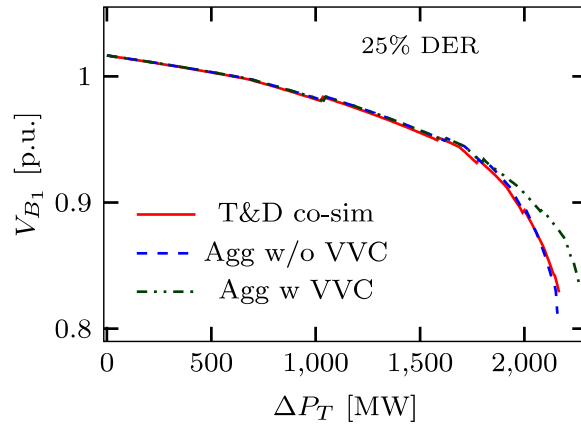


Figure 4.17 HV side voltage for 25% DER scenario.

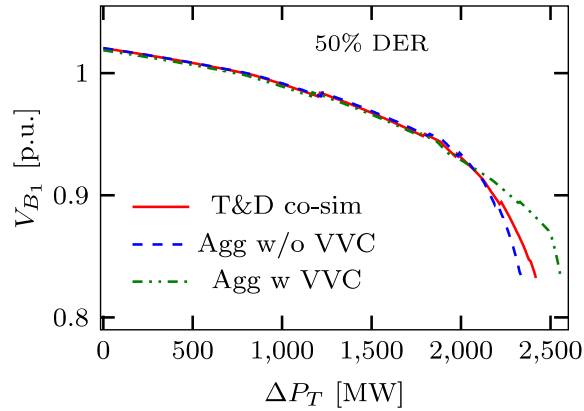


Figure 4.18 HV side voltage for 50% DER scenario.

Table 4.12 presents the maximum ΔP_T across different DER scenarios, indicating that the initial power at the T&D interface significantly decreases when compared to constant impedance loads. Notably, the maximum ΔP_T experiences a substantial reduction in scenarios with no DER. Furthermore, the aggregated model without VVC appears to provide a close, albeit conservative, estimate of the margin relative to T&D co-simulation results.

Table 4.12 Max. ΔP_T [in MW] from different studies with constant power loads

Type of Study	No DER		25% DER		50% DER	
	P_{T_o}	Max P_T	P_{T_o}	Max P_T	P_{T_o}	Max ΔP_T
T&D co-sim	936	1913	693	2166	462	2419
Agg.Model w/o VVC	936	1974	693	2158	462	2347
Agg.Model w VVC	—	—	693	2263	462	2553

The reactive power injection in the aggregated model with VVC results in an overestimated transferability limit. With constant power load models and higher DER proliferation in the distribution network, the aggregated model without VVC provides a conservative analysis. In contrast, the aggregated model with VVC yields an overly optimized estimate, which may be problematic from a planning perspective. This highlights the need for careful selection of modeling approaches to ensure accurate assessments of transfer capabilities.

5. Conclusions

This work quantifies the impact of IBRs on voltage stability assessments and demonstrates how the transferability of transmission and distribution (T&D) systems is affected by increased IBR proliferation. IBRs with VVC significantly enhance the system's transfer margin, making it crucial to understand how IBR capabilities alter power flows across T&D interfaces. The most accurate transfer margin is derived from T&D co-simulation, due to the detailed modeling of the distribution network. Thus, this study highlights the effectiveness of aggregated models in capturing the transferability margin under high levels of DER proliferation and evaluates whether these models require upgrades.

The following are the conclusions drawn from the analysis:

1. The effectiveness of the T&D co-simulation framework relies on the granularity of the model, necessitating a complete footprint of the distribution network and its hosting capability. To address uncertainties, Monte Carlo studies can be employed; however, it is essential to understand the extent to which modeling uncertainties impact transferability assessments. Furthermore, the strength of the distribution network is crucial for accurately estimating stability margins using co-simulation.
2. The detailed modeling of the distribution network within the T&D co-simulation framework enables the capture of all aspects of the distribution system. This comprehensive approach allows for accurate estimation of the true transfer margin under various DER penetration scenarios. Additionally, VVC enhances the distribution system's load-handling capability, leading to increased transferability as the system approaches the nose point of the PV curve.
3. Aggregated models (without VVC) used in stability studies approximate the transfer margin closely to that of the T&D co-simulation. Despite the variety of load models present in the distribution network, the constant PQ load representation in the aggregated model sufficiently captures the transfer margin under different DER penetration levels. While the estimated margin may vary, it typically remains within the ballpark of the true margin.
4. The inclusion of VAR support in aggregated models (with VVC) often leads to overly optimistic results, which can be detrimental from a planning perspective as it creates a false sense of security. The oversimplified model with VVC tends to generate higher reactive power injection, raising concerns about whether the IBRs in the distribution system are providing full VAR support for the given loading conditions. However, a notable advantage of aggregated models with VVC is their ability to achieve better voltage alignment with T&D co-simulation results under higher DER penetrations.

5.1 Guidelines for Performing Voltage Stability Assessment

Based on our comprehensive analysis of various test systems, we have developed the following guidelines for conducting stability assessments in IBR-rich grids:

1. Connect low-voltage distribution buses to transmission buses via a transformer using aggregated models for stability studies.
2. Represent net load of the distribution network as constant PQ loads (S_{nl}) at distribution buses in the aggregated models.

3. Model capacitance and DER injections in the distribution network as constant reactive power (Q_{sh}) and constant PQ power (S_{DER}) injections for stability studies.
4. Conduct an initial T&D co-simulation to establish nominal parameters (S_{nl} , Q_{sh} , and S_{DER}). These can also be derived from transmission bus measurement data.
5. Increment S_{nl} linearly ($P_{nl}(1 + \lambda) + jQ_{nl}(1 + \lambda)$), where λ is the load increment parameter. Maintain Q_{sh} and S_{DER} as fixed during the stability assessment.
6. Use the aggregated model without voltage and var control (VVC) to capture the system's transfer margin; results may be conservative or optimistic but typically reflect the true margin.
7. The aggregated model with VVC often produces optimistic estimates for the transfer margin, with Q_{DER} injected based on a lookup table derived from distribution system data.
8. For transmission operators seeking voltage magnitudes above 0.9 p.u., the aggregated model with VVC is advisable, offering improved transmission voltage and transferability margins.

5.2 Future Work

The present study conducts a comparative analysis of co-simulation frameworks and aggregated models for assessing stability in IBR-dominated grids. Based on this analysis, the following future research directions are proposed:

1. Further investigation is needed on the effects of IBRs on voltage stability assessments, incorporating the uncertainties of these resources within realistic distribution networks. This study should clarify the extent to which IBR uncertainties should be included in planning studies and how they can be effectively represented in aggregated models for stability assessments.
2. The interaction between load models and the strength of the distribution system directly influences the stability of transmission and distribution (T&D) systems. A systematic analysis is required to explore how various load model combinations and system strengths affect voltage stability. This analysis should leverage statistical correlations with existing data, and the findings must be integrated into the aggregated models used for bulk power grid stability assessments.
3. Enhancements are needed in the parameterization of aggregated models to accurately represent the VVC of IBRs. The models should produce results that align closely with transfer margin estimates derived from the T&D co-simulation framework. One potential improvement is to incorporate a distribution equivalent feeder to account for losses in the distribution network.
4. The current study emphasizes steady-state voltage stability under higher IBR penetrations. Future research should also address dynamic voltage stability and explore potential correlations between dynamic and static stability assessments. These studies should serve as a foundation for translating insights from simpler models into more complex dynamic frameworks.

Appendix A Comparison with TDcoSim

The code developed for transmission and distribution (T&D) co-simulation has been rigorously validated through comparison with TDcoSim [32], a sophisticated co-simulation tool developed by Argonne National Laboratories. TDcoSim is a Python package designed to facilitate comprehensive co-simulations that integrate a transmission system simulator (TSS), multiple distribution system simulator (DSS) instances, and various solar PV-DERs.

This tool enables both static and dynamic co-simulations for power system models featuring hundreds of transmission buses, distribution feeder nodes, and DERs. Users configure TDcoSim via a configuration file, where they specify the desired transmission system, distribution system, and the type of simulation, either static or dynamic. The package utilizes PSS/E for transmission system analysis and OpenDSS for distribution network evaluation. Notably, the static configuration option allows for the definition of load shapes, which can be used to incrementally load the distribution system.

To validate the developed code, we have conducted case studies using the IEEE 9-bus and a relaxed IEEE 123 distribution system. This comprehensive validation process ensures the reliability and accuracy of the co-simulation results.

1. Case-A: One D-system with NO DER at Bus 7 of transmission Bus, with transformer reactance (X_{tf}) of 0.1 p.u. at T&D interface.
2. Case-B: One D-system with NO DER at Bus 7 of transmission Bus, with transformer reactance (X_{tf}) of 0.01 p.u. at T&D interface.
3. Case-C: Multiple D-systems with 25% DER penetration. Bus 7 and 5 are considered for analysis.

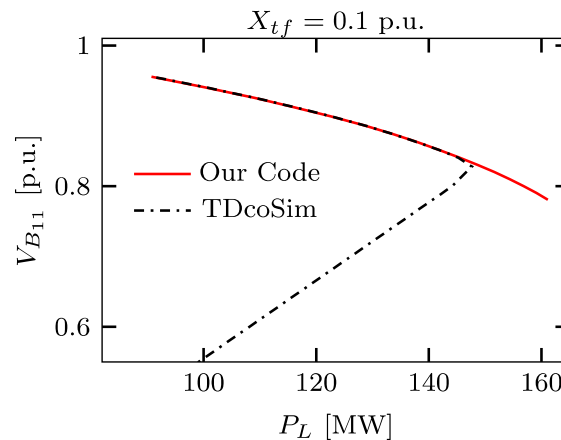


Figure A.1. PV curve corresponding to Case-A.

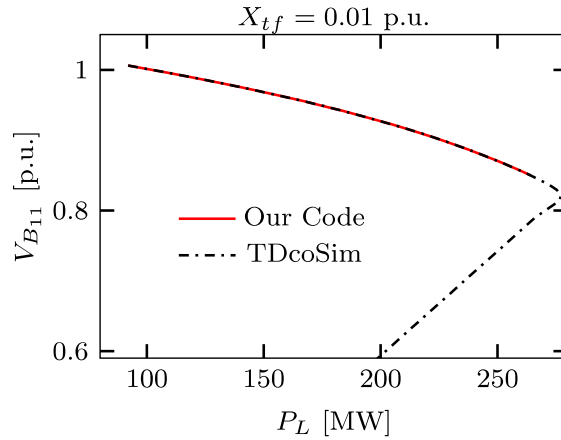


Figure A.2 PV curve corresponding to Case-B.

The PV curves for Case A and Case B are illustrated in Figure A.1 and Figure A.2, respectively. The transformer reactance results in a notable voltage drop at the distribution system interface bus; a lower transformer reactance significantly enhances power transfer. Furthermore, the developed code aligns closely with TDcoSim under the scenario without DERs.

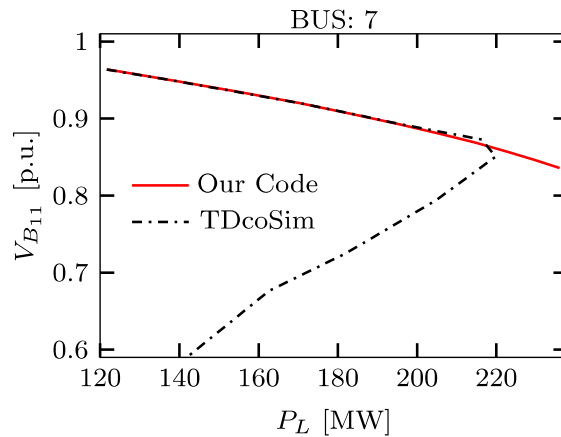


Figure A.3 PV curve corresponding to Case-C at Bus 7.

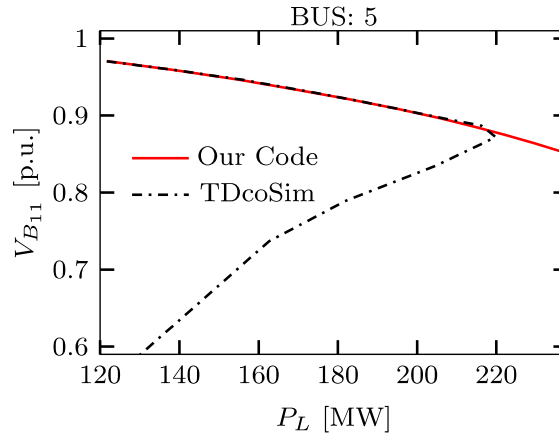


Figure A.4 PV curve corresponding to Case-C at Bus 5.

DERs were integrated into the distribution system using OpenDSS. The typical PV curve observed under a 25% DER scenario is depicted in Figure A.3 and Figure A.4, demonstrating that the developed code effectively captures the nose point. The correlation with TDcoSim further validates the correctness of the algorithm implemented for stability assessment. Additionally, Figure A.3 and Figure A.4 indicate that the inclusion of DERs substantially improves the transfer margin.

Appendix B Strengthening of Distribution Networks for Stability Studies

Distribution networks are essential for transmitting electrical power from transmission systems to end users, including residential and industrial customers. These systems are designed to effectively meet expected average load demands while accommodating future growth without exceeding established limits. These limits include equipment capacity ratings, voltage thresholds, and safety margins that ensure reliable operation of the system. However, it is important to note that distribution systems are not inherently designed for stability studies. As a result, they may not adequately address the increasing load demands encountered during stability assessments, particularly when facing higher load increments.

To accommodate rising electrical consumption, it is essential to modernize the distribution system. This modernization may involve increasing capacity, enhancing voltage regulation, and adding feeders to address future load demands. Such improvements facilitate effective management of varying loading conditions and strengthen the system's capacity to support comprehensive stability assessments. Given that generating case data for each loading scenario with these enhancements is impractical, we propose strengthening of the distribution networks.

Let us examine the PV curve, as illustrated in Figure B.1, for the IEEE 9-bus system alongside the unstrengthened IEEE 123 node distribution network, which operates without any DERs.

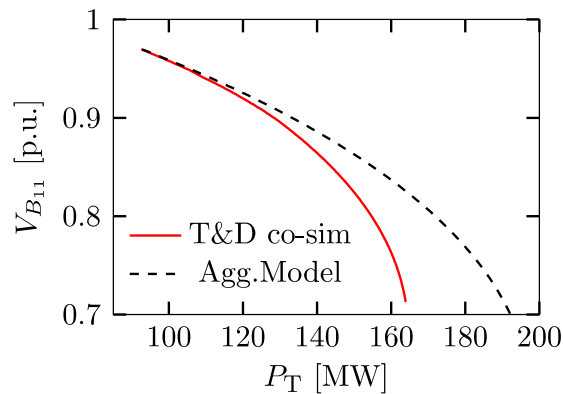


Figure B.1 PV Curve for the IEEE 9-bus system and unstrengthened IEEE 123 node distribution network.

It is well established that T&D co-simulation accurately captures the transfer margin. However, comparisons with aggregated models reveal a significant discrepancy of 40 MW in scenarios without DERs. This difference is concerning, as conventional aggregated models used in planning studies have historically provided reliable assessments. If such a substantial discrepancy existed, the power system would likely have faced significant voltage instability and blackouts. Additionally, upgrades to these aggregated models would have been implemented to maintain reliability in assessments.

Given this context, the critical question we now face is: how can we trust the aggregated models with such a difference when incorporating the behavior of IBRs for stability assessments? For this purpose, we propose the strengthening of the distribution network to perform stability assessments.

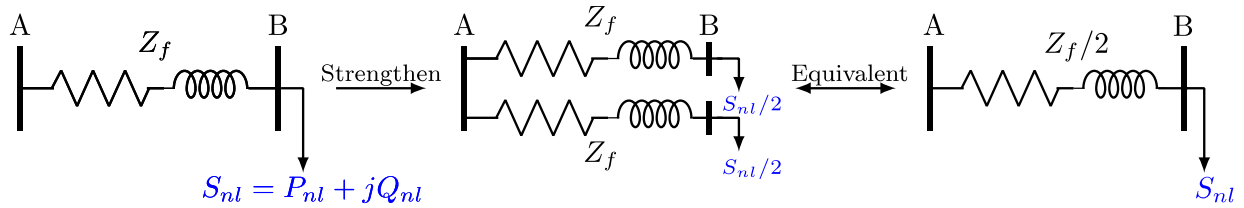


Figure B.2 Strengthening of the distribution network for stability studies.

The key concept behind strengthening the distribution system is illustrated in Figure B.2. Consider a feeder impedance Z_f between distribution buses A and B, with a load S_{nl} at bus B. Under normal conditions, the entire load current required to meet the demand S_{nl} flows through Z_f . By strengthening the system, we can effectively split S_{nl} into two equal parts, reducing the load at bus B that passes through Z_f . This approach enhances the voltage operating range and allows for increased loading conditions. Additionally, an alternative method shown in Figure B.2 involves reducing the feeder impedance while keeping the load S_{nl} at bus B unchanged. This strategy also reduces losses and provides greater flexibility for load increments.

References

- [1] P. Kundur *et al.*, "Definition and classification of power system stability IEEE/CIGRE joint task force on stability terms and definitions," in *IEEE Transactions on Power Systems*, vol. 19, no. 3, pp. 1387-1401, Aug. 2004, doi: 10.1109/TPWRS.2004.825981.
- [2] N. Hatziargyriou *et al.*, "Definition and Classification of Power System Stability – Revisited & Extended," in *IEEE Transactions on Power Systems*, vol. 36, no. 4, pp. 3271-3281, July 2021, doi: 10.1109/TPWRS.2020.3041774.
- [3] P. Kundur, *Power System Stability*, 2007.
- [4] P. W. Sauer and M. A. Pai, "Power system steady-state stability and the load-flow Jacobian," in *IEEE Transactions on Power Systems*, vol. 5, no. 4, pp. 1374-1383, Nov. 1990, doi: 10.1109/59.99389.
- [5] T. Van Cutsem and C. Vournas, *Voltage stability of electric power systems*, Springer Science and Business Media, 2007.
- [6] MISO, "MISO's Renewable Integration Impact Assessment (RIIA)," 2021.
- [7] "IEEE Standard for Interconnection and Interoperability of Distributed Energy Resources with Associated Electric Power Systems Interfaces," IEEE Std 1547-2018 (Revision of IEEE Std 1547-2003), pp. 1-138, 2018.
- [8] NERC, "Distributed Energy Resources Connection Modeling and Reliability Considerations," 2017.
- [9] NERC Reliability Guidelines, "BPS-Connected Inverter-Based Resource Performance," 2018.
- [10] EPRI, "Adequacy of Voltage Stability Methodologies for System with Large Integration of IBRs," EPRI, Palo Alto, CA, 2022.
- [11] H. P. Lee, K. Dsouza, K. Chen, N. Lu and M. E. Baran, "Adopting Dynamic VAR Compensators to Mitigate PV Impacts on Unbalanced Distribution Systems," in *IEEE Access*, vol. 11, pp. 101514-101524, 2023, doi: 10.1109/ACCESS.2023.3315601.
- [12] EPRI, "Voltage Control and Reactive Power Management: Reference Guide - Industry Practices and Tools for Voltage/Var Planning and Management (VVPM)," EPRI, Palo Alto, CA, 2022.
- [13] V. Ajjarapu, *Computational Techniques for Voltage Stability Assessment and Control*, Springer Science Business Media, LLC, 2006.
- [14] S. (NDR) Nuthalapati, *Use of Voltage Stability Assessment and Transient Stability Assessment Tools in Grid Operations*, Springer Nature, Switzerland, 2021.
- [15] EPRI, "Program on Technology Innovation: Online Power System Stability Assessment Using Real-Time Measurements", EPRI, Palo Alto, CA, 2010.
- [16] J. Rueda-Torres, E. Hillberg, V. Ajjarapu, *et al.*, "Evaluation of Voltage Stability Assessment Methodologies in Transmission Systems: TR 109", IEEE, 2023.
- [17] A. R. R. Matavalam, S. M. H. Rizvi, A. K. Srivastava and V. Ajjarapu, "Critical Comparative Analysis of Measurement Based Centralized Online Voltage Stability Indices," in *IEEE Transactions on Power Systems*, vol. 37, no. 6, pp. 4618-4629, Nov. 2022, doi: 10.1109/TPWRS.2022.3145466.
- [18] B. Milosevic and M. Begovic, "Voltage-stability protection and control using a wide-area network of phasor measurements," in *IEEE Transactions on Power Systems*, vol. 18, no. 1, pp. 121-127, Feb. 2003, doi: 10.1109/TPWRS.2002.805018.

- [19] A. R. Ramapuram Matavalam, A. Singhal and V. Ajjarapu, "Monitoring Long Term Voltage Instability Due to Distribution and Transmission Interaction Using Unbalanced μ PMU and PMU Measurements," in *IEEE Transactions on Smart Grid*, vol. 11, no. 1, pp. 873-883, Jan. 2020, doi: 10.1109/TSG.2019.2917676.
- [20] F. Hu, K. Sun, A. Del Rosso, E. Farantatos and N. Bhatt, "Measurement-Based Real-Time Voltage Stability Monitoring for Load Areas," in *IEEE Transactions on Power Systems*, vol. 31, no. 4, pp. 2787-2798, July 2016, doi: 10.1109/TPWRS.2015.2477080.
- [21] D. Q. Zhou, U. D. Annakkage and A. D. Rajapakse, "Online Monitoring of Voltage Stability Margin Using an Artificial Neural Network," in *IEEE Transactions on Power Systems*, vol. 25, no. 3, pp. 1566-1574, Aug. 2010, doi: 10.1109/TPWRS.2009.2038059.
- [22] C. Zheng, V. Malbasa and M. Kezunovic, "Regression tree for stability margin prediction using synchrophasor measurements," in *IEEE Transactions on Power Systems*, vol. 28, no. 2, pp. 1978-1987, May 2013, doi: 10.1109/TPWRS.2012.2220988.
- [23] H. -Y. Su and T. -Y. Liu, "Enhanced-Online-Random-Forest Model for Static Voltage Stability Assessment Using Wide Area Measurements," in *IEEE Transactions on Power Systems*, vol. 33, no. 6, pp. 6696-6704, Nov. 2018, doi: 10.1109/TPWRS.2018.2849717.
- [24] V. Ajjarapu and C. Christy, "The continuation power flow: a tool for steady state voltage stability analysis," in *IEEE Transactions on Power Systems*, vol. 7, no. 1, pp. 416-423, Feb. 1992, doi: 10.1109/59.141737.
- [25] Y. Wang *et al.*, "Voltage Stability Monitoring Based on the Concept of Coupled Single-Port Circuit," in *IEEE Transactions on Power Systems*, vol. 26, no. 4, pp. 2154-2163, Nov. 2011, doi: 10.1109/TPWRS.2011.2154366.
- [26] EPRI, "Identification of Voltage Collapse Point in P-V Analysis", EPRI, Palo Alto, CA, 2016.
- [27] P. Aristidou, G. Valverde and T. Van Cutsem, "Contribution of Distribution Network Control to Voltage Stability: A Case Study," in *IEEE Transactions on Smart Grid*, vol. 8, no. 1, pp. 106-116, Jan. 2017, doi: 10.1109/TSG.2015.2474815.
- [28] L. R. de Araujo, D. R. R. Penido, J. L. R. Pereira and S. Carneiro, "Voltage Security Assessment on Unbalanced Multiphase Distribution Systems," in *IEEE Transactions on Power Systems*, vol. 30, no. 6, pp. 3201-3208, Nov. 2015, doi: 10.1109/TPWRS.2014.2370098.
- [29] A. K. Bharati and V. Ajjarapu, "Investigation of Relevant Distribution System Representation With DG for Voltage Stability Margin Assessment," in *IEEE Transactions on Power Systems*, vol. 35, no. 3, pp. 2072-2081, May 2020.
- [30] S. M. H. Rizvi and A. K. Srivastava, "Integrated T&D Voltage Stability Assessment Considering Impact of DERs and Distribution Network Topology," in *IEEE Access*, vol. 11, pp. 14702-14714, 2023, doi: 10.1109/ACCESS.2023.3243100.
- [31] K. Anderson, J. Du, A. Narayan and A. E. Gamal, "GridSpice: A Distributed Simulation Platform for the Smart Grid," in *IEEE Transactions on Industrial Informatics*, vol. 10, no. 4, pp. 2354-2363, Nov. 2014, doi: 10.1109/TII.2014.2332115.
- [32] K. Balasubramaniam *et al.*, "Co-Simulation of Transmission and Distribution Systems—From Modeling to Software Development," in *IEEE Access*, vol. 10, pp. 127061-127072, 2022, doi: 10.1109/ACCESS.2022.3224939.
- [33] EPRI, "Modeling High-Penetration PV for Distribution Interconnection Studies: Smart Inverter Function Modeling in OpenDSS, Rev 3", EPRI, Palo Alto, CA, 2017.

- [34] Illinois Center for a Smarter Electric Grid, "Online," 2013. [Online]. Available: <http://publish.illinois.edu/smartergrid/>.
- [35] Wang, Bin, Richard Wallace Kenyon, and Jin Tan. 2022. Developing a PSCAD Model of the Reduced 240-Bus WECC Test System: Preprint. Golden, CO: National Renewable Energy Laboratory. NREL/CP-6A40-82287. <https://www.nrel.gov/docs/fy22osti/82287.pdf>